UNIVERSITY OF CINCINNATI

Date: 5/26/04

I, Justin R. Sipes

hereby submit this work as part of the requirements for the degree of:

Master of Science

in:

Mechanical Engineering

It is entitled:

Optimal Design of a Pneumatically Adhered Sensor Attachment Device

This work and its defense approved by:

Chair: David F. Thompson

Randall J. Allemang

Robert W. Rost

Optimal Design of a Pneumatically Adhered Sensor Attachment Device

A thesis submitted to the
Division of Research and Advanced Studies
of the University of Cincinnati

in partial fulfillment of the
requirements for the Degree of

MASTER OF SCIENCE

From the Department of Mechanical, Industrial and Nuclear Engineering
of the College of Engineering

2004

by

Justin R. Sipes

B.S.M.E., University of Cincinnati, 2002

Committee Chair: David F. Thompson, PhD

Abstract

In vibrations testing, a structures response to a vibratory excitation is quantified and analyzed. A vibratory excitation is often generated by an electro-dynamic shaker, which is attached to the test structure. The attachment of the electro-dynamic shaker to the test structure usually requires the modification of the structures surface or the adhesive attachment of a threaded mounting base to the structure's surface.

Often in automotive applications, where an automobile's dynamic characteristics are being analyzed, damage to the surface of the test structure is clearly undesirable. To address this, a pneumatic shaker attachment fixture was designed by test engineers that coupled a shaker to a test structure by vacuum. The design of the device was successful, but an in-depth analysis of its performance was not carried out.

To augment the design of the device, its design was numerically optimized using a conventional gradient-based constrained minimization algorithm within MATLAB. In the optimization, the fixture's mass was minimized while subject to performance and manufacturing constraints.

Through design optimization, the fixture's mass was reduced by 66%. To evaluate the performance of the attachment fixture, the frequency response of a structure was measured using a current method of shaker attachment and compared to a frequency response measurement of the same structure when using the pneumatic attachment fixture.

The measured dynamics of the test setup using the attachment fixture were noted to be quite different than those of the test setup using a conventional shaker attachment method. The source of the difference was explored by varying design parameters and by finite element modeling, and was determined to be dependant on several different factors.

The result of this work is a lightweight means of coupling a shaker to a test structure suitable for low frequency vibration testing. Surface damage to the test structure caused by shaker mounting is minimized and the test engineer is able to easily reposition the shaker during testing.

Acknowledgements

I would like to thank the many people who made this project possible. First, my thesis committee: Dr. Thompson, Dr. Allemang, and Dr. Rost. Their continual guidance and support proved to be vital to this project's completion.

I would like to thank Dr. Thompson, my advisor, for many hours of his time discussing both this project and my academic interests.

I would like to thank all of the students and staff of the Structural Dynamics Research Laboratory for their support. Special thanks to Dr. Allemang, Jim Parker and Ray Martell for their assistance and guidance with the experimental evaluation of this project.

I would like to thank my family for providing me the means and instilling the desire to pursue an education.

Lastly, I thank my fiancée, Nisha Schuler, for her support. Nisha was a continual source of motivation in the completion of this work.

Table of Contents

List of Figures

List of Tables

Chapter 1 - Introduction

In experimental modal analysis, a structure's reaction to a vibratory excitation is quantified and analyzed. There are different ways of subjecting a test structure to a vibratory excitation: external sources such as mechanical impact or electro-dynamic shaker excitation, or internal sources occurring during the normal operation of the machine or structure, such as rotating unbalance. In shaker excitation, the method considered in this thesis, a traditional method of transmitting the shaker's excitation to the structure is by means of a long thin rod, or "stinger." The stinger is designed to be axially stiff, so as to transmit the force generated by the shaker, but to be compliant in bending to impart as little effect as possible on the vibrating structure or the exciter.

In connecting the stinger to a test structure, two methods are common. The first typical method of attachment involves the bonding of a threaded base to the structure through the use of an adhesive such as cyanoacrylate or dental cement. The use of these adhesives can be troublesome in certain applications, especially where the surface finish of the test structure is to be preserved. The application of these adhesives or their subsequent removal at the conclusion of testing can damage the test structure's surface, be it paint damage or surface scratching. Along with surface damage, other consequences of using adhesive-bonded threaded bases include the inability to quickly reposition the base and the possibility of misalignment due to inconsistent adhesive layer thickness under the base. The second common method of attachment is to directly thread a base into a threaded hole made in the structure. This method is clearly undesirable when there is concern about damaging the surface of the test structure.

To address these issues, a pneumatically adhered attachment fixture to connect a shaker to a test structure was designed by vibrations engineers. The device consisted of a metallic vacuum chamber, or "cup," separated from atmospheric pressure by a toroidal rubber seal, or o-ring. A small pressure tap was located radially outward from the center of the cup, which was connected by rubber tubing to a vacuum pump. The pump provided a pressure differential over the area of the seal, yielding a resultant load that acted to clamp the device to a test structure.

The design of the attachment fixture was both simple and functional, but an in-depth analysis of the device's desired performance was not carried out during the design due to time and cost. This thesis attempts to augment the design of the attachment fixture so as to improve its performance through numerical design optimization.

Design optimization has proved to be an invaluable tool at engineers' disposal in product development. It can facilitate a product development cycle comprising of efficiency in both financial terms and in terms of a minimal development cycle lifespan. Product design and development cycles can be shortened due to a reduction of the reiteration of traditional "guess and check" design methodologies employed in the past. Optimization can enable a designer to convert a product concept into a functionally "optimal" form while investing a minimal amount of resources **[1], [2].**

The foundations of optimization are well documented in textbooks written by Arora **[1]**, Papalambros and Wilde **[3]**, and Rao **[4]**. Optimal design principles, having long been developed, have been recently empowered by the digital computer. With the recent advances in computing power, engineers have been enabled to address more numerically complex optimization projects than have been possible in the past.

The use of optimization in industry is wide spread and has been employed in the design of countless machines and systems. The concept of design optimality can be applied to most engineering design pursuits. A broad group of examples of optimization in different design contexts are given by **[5], [6], [7], [8], [9]**. Optimization can be implemented to reduce or increase, as the application dictates, almost any quantifiable parameter of a design of an object or system.

An important fact to note, as evidenced by this thesis, is that a solution determined by numerical optimization is only accurate when the analytical model of the system being designed is accurate. An optimized design solution is of little consequence if it stems from a model that fails to capture the true physical behavior of the system in question. Care must be taken in the preliminary modeling steps of the problem to ensure the accuracy of the optimized solution.

With careful use, design optimization provides designers with an indispensable aid in engineering design problems. This thesis develops a design methodology of a pneumatically adhered shaker attachment device. A gradient-based constrained

minimization algorithm within the Optimization Toolbox of MATLAB is used to minimize the mass of said system while simultaneously satisfying design and performance constraints. Once the optimized solution was obtained, a prototype was fabricated and functionally evaluated.

Chapter 2 - Definitions and Assumptions

2.1 Preliminary Design Considerations

Figure 1 defines the general design of the attachment fixture.

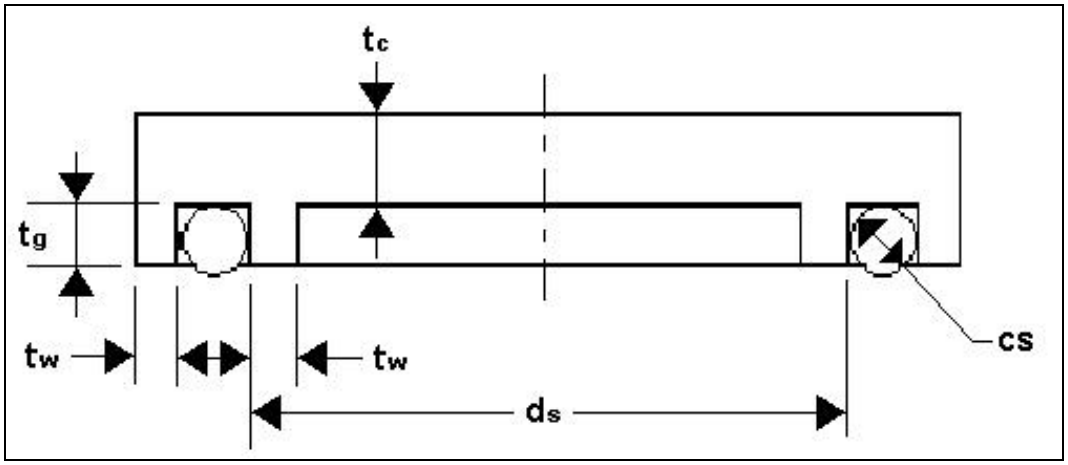

Figure 1. General Design of Attachment Fixture

Where t_c is the cup thickness, t_w, is the wall thickness, t_g is the gland thickness, d_s is the seal diameter, and cs is the cross section diameter of the seal. This general design best estimates the existing design as developed by engineers for use in modal testing in the aerospace industry. Material selection for the attachment fixture was essentially arbitrary, but aluminum 6061-T6 was chosen as the cup material because of its past success in the previous design and its desirable material properties, namely its inherent low density, high rigidity, and its machinability. By assuming this form, the performance improvement made by the numerical optimization can be best quantified and studied. The seal material was chosen to be nitrile rubber with a Shore "A" scale hardness of 50. A soft elastomer compound can be chosen due to the presence of a relatively low pressure differential (15 psi max) in this application **[10]**. By choosing a relatively "soft" rubber compound, the force needed to compress the seal to its working height is reduced, therefore allowing for a more compact design.

2.2 Load Considerations

To pneumatically mount an electrodynamic vibration generator, or shaker, to a specimen in vibration testing, a number of physical considerations must be addressed and understood. The means of coupling the attachment fixture to the test structure is the resulting load from an applied pressure differential across the sealing area of the device. The pressure differential in this application is generated by a vacuum pump, which evacuates the chamber formed by the interface of the attachment fixture and the test specimen. The effective area is defined as the mean diameter of the toroidal seal. Figure 2 shows the generalized loading condition of the attachment fixture.

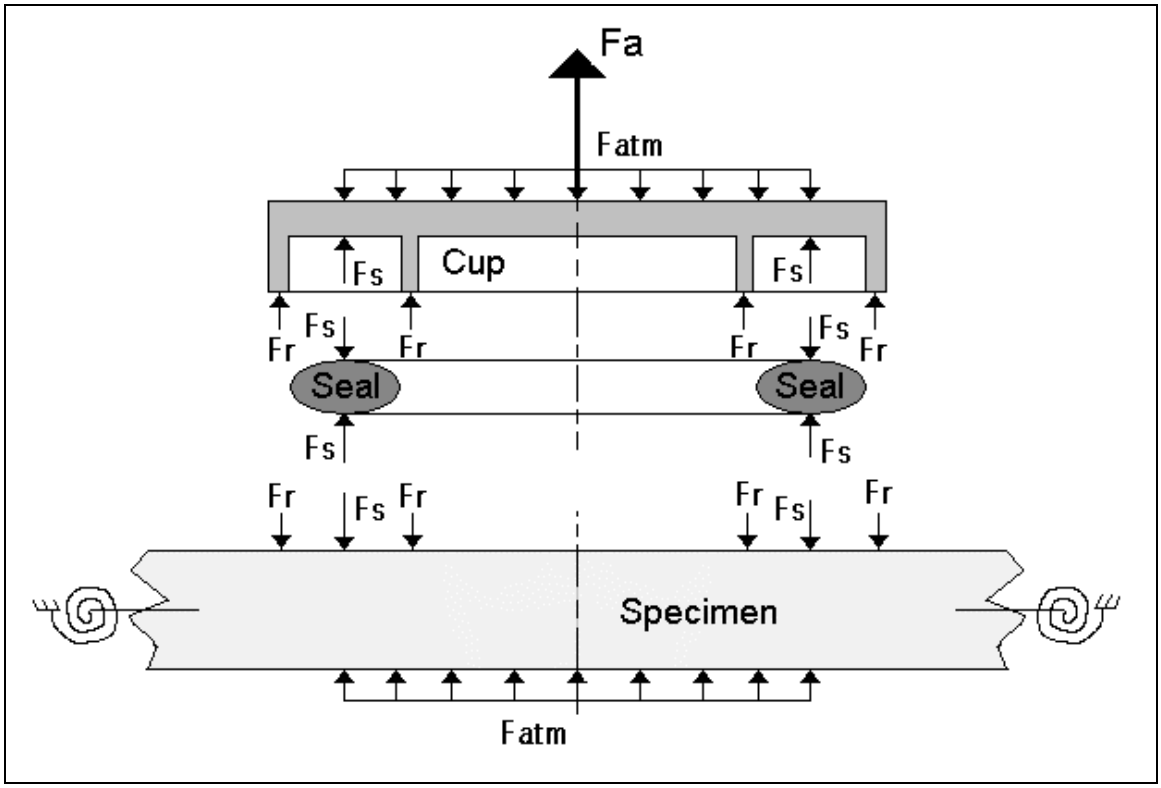

Figure 2. Generalized Loading Condition of the Attachment Fixture

To analyze the system, a free body diagram can be analyzed for each of the bodies in the cup – seal – specimen interface. The forces, with respect to the cup, are outlined below:

F_a is the external force applied by the shaker to the system.

F_{atm} is the force of the vacuum acting on the area of the seal.

F_s is the force exerted by the compressed seal on the cup.

F_r is the reaction force of the specimen on the cup. This force is equal in magnitude and opposite in direction to the normal force exerted by the cup on the specimen.

The normal force of the cup acting on the specimen is equal to the resultant of F_{atm} added to F_s. The seal compression force, F_s, is determined by the product of the seal circumference and the seal compression load per unit length. The seal compression load is a function of the seal compression percentage and the seal cross sectional diameter, and therefore varies for each iterated design vector in the optimization. Data for the seal compression load for different cross-sectional diameters and deformations are published in **[10]**.

Looking at the cup in static equilibrium (without external forces), the forces must sum to zero. Thus:

$$F_{atm} + (-F_s) + (-F_r) = 0 \qquad (\mathbf{1})$$

The addition of the external force F_a yields:

$$F_{atm} + (-F_s) + (-F_r) + (-F_a) = 0 \quad (\mathbf{2})$$

When external force F_a is introduced to the system in the direction such that the cup is being pulled from the specimen, because F_{atm} and F_s are fixed for a given design vector, F_r varies with F_a. When the magnitude of F_a is increased to the point at which F_r reaches

zero, the cup separates from the specimen and relative motion between the cup and specimen is allowed. It is assumed the cup does not move relative to the specimen if the following inequality is satisfied:

$$F_{atm} + (- F_s) + (- F_a) = (F_r)_{worst\ case} \geq 0 \qquad (3)$$

The load considerations for an arbitrarily selected design configuration are visualized in the force diagram in Figure 3:

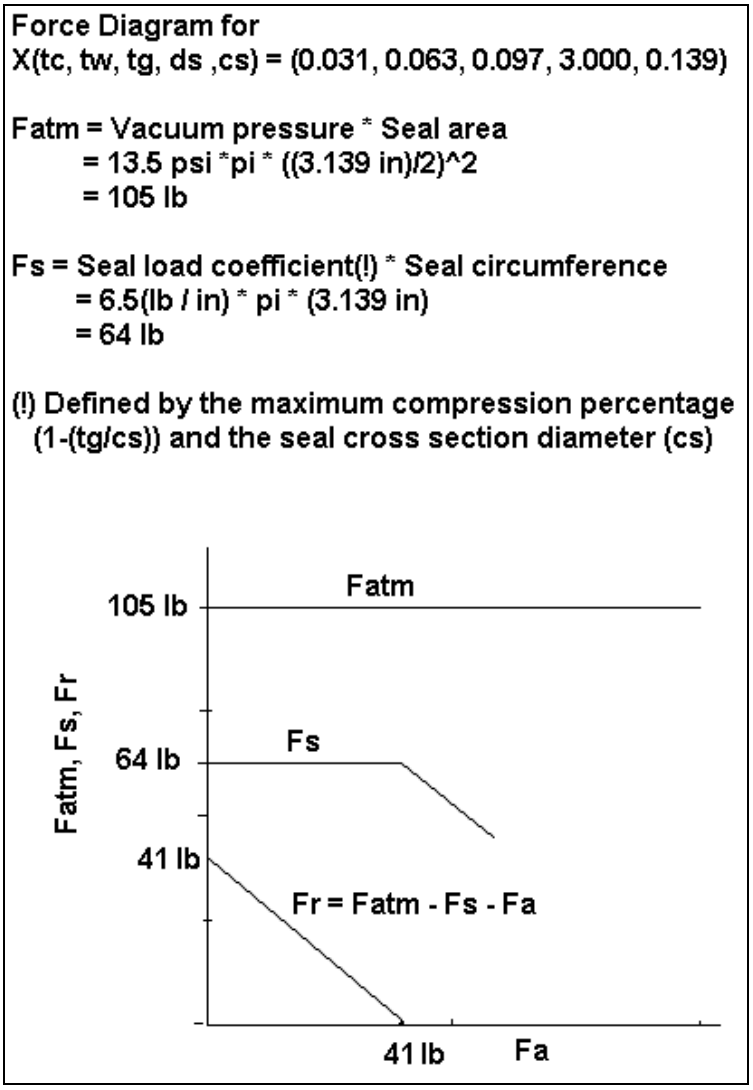

Figure 3. Force Diagram for Arbitrarily Chosen Design Vector

In Figure 3 above, it is shown that as F_a is increased to 41 (lb) for this design vector, F_r reaches zero and relative motion is allowed.

2.3 Mounting Geometry Considerations

In the design of the mounting fixture, two different mounting surface conditions are considered. First, in a flat surface mounting condition, the seal is compressed until the cup makes contact with the test structure around the entire circumference of the cup, as shown in Figure 4.

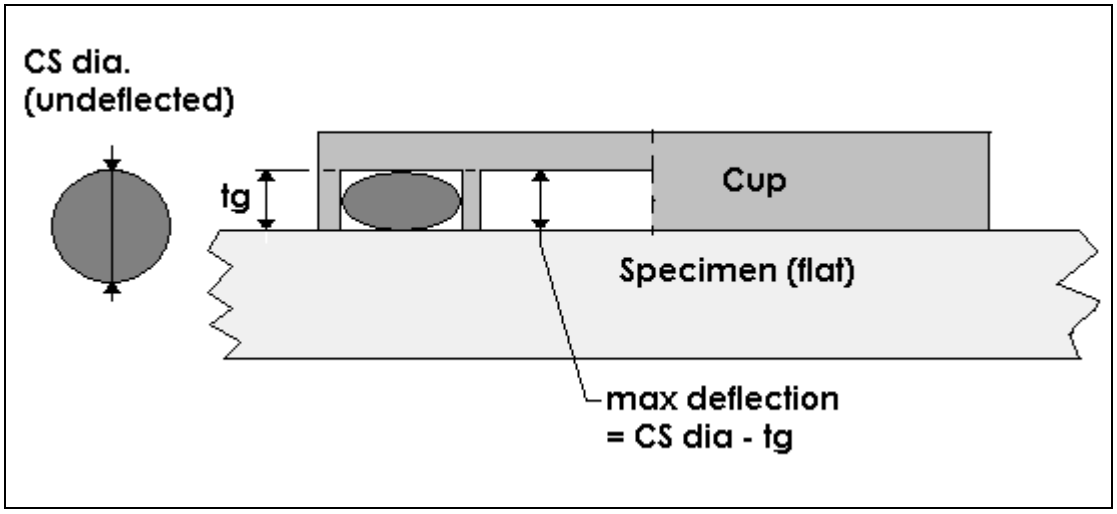

Figure 4. Flat Mounting Condition Diagram

The amount of seal compression is dependent on the constituents of the design vector, namely gland thickness, t_g, and the seal cross-section diameter, cs. The seal compression percentage is given by:

$$\text{Seal compression (\%)} = 1 - \frac{t_g}{cs} \qquad (4)$$

The second mounting surface consideration is that of a cylindrical or curved surface. Because the attachment fixture will be used to perform tests on vehicles, it needs to be

able to mount to slightly curved surfaces, common occurrences on modern vehicles. When mounted to a curved surface, the entire circumference of the cup does not come in contact with the specimen, causing the seal compression percentage to vary around the circumference of the seal.

The maximum seal compression for the curved surface mounting condition is still a function of the design vector, **x**; namely the gland thickness, t_g, and the seal cross-sectional diameter, cs, just as defined in equation (**4**) for the flat surface mounting condition. Thus, the maximum seal compression percentage for the curved mounting condition is equal to that of the seal compression percentage calculated for the flat surface mounting for any given design vector.

When mounted to a curved surface, the seal compressive force, F_s, can be assumed to be less than when the fixture is mounted to a flat surface. Because the seal compression varies around the circumference of the seal-specimen interface and the maximum seal compression is still defined as it is in a flat surface mounting condition by the design vector, **x**, the seal compression force, F_s, for a curved surface orientation is always less than that of a flat surface mounting orientation for any design vector, **x**.

The minimum seal compression is dependent on geometry of the cup, the seal, and the test specimen. The minimum seal compression percentage is given by:

$$\text{Minimum compression percentage} = \frac{cs - t_g - h}{cs} \qquad (\mathbf{5})$$

The variable h represents the height of the chord made by the contact points of the seal and the specimen at the two points of minimum seal compression. In Figure 5 below, chord height h is further developed. Chord height h is given by:

$$h = R_{min}(1 - \cos(\frac{\theta}{2})) \qquad \textbf{(6)}$$

Where:

$$\theta = \frac{(d_s + cs)}{2} * \frac{1}{R_{min}} \qquad \textbf{(7)}$$

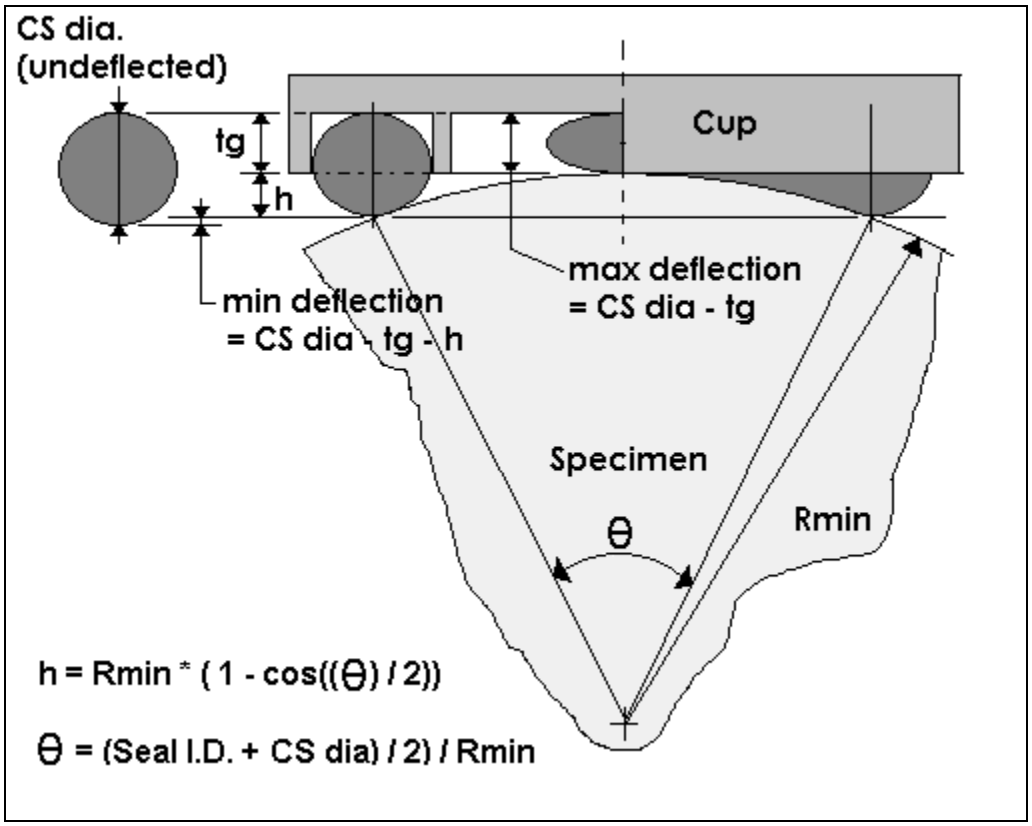

Figure 5. Curved Mounting Condition Geometry Considerations

For this design, the minimum radius of curvature of a curved test specimen, R_{min}, was arbitrarily chosen to be 0.75 (m) or roughly 30 (in).

The assumed material and physical constants used in the design optimization are given in Table 1.

Symbol	Constant / Property	Value	Units
ρ_c	Cup material density	2710	(kg/m^3)
ρ_s	Seal material density	910	(kg/m^3)
Ec	Cup material elastic modulus	71	(GPa)
υ	Cup material Poisson's Ratio	0.33	-
R_{min}	Minimum curvature radius	0.75	(m)
p_{vac}	Obtainable vacuum	93000	(Pa)
$M_{armature,\ stinger}$	Shaker armature and stinger mass	0.218	(kg)
$F_{applied,\ max}$	Maximum applied excitation force	135	(N)

Table 1. Physical and Material Constants

2.4 Modal Analysis Considerations

In designing a device for use in the field of experimental modal analysis, several factors must be considered. To ensure experimental accuracy, the test setup should influence the system of interest as minimally as possible.

The excitation of a structure is traditionally quantified by a force measurement taken by a load transducer located in between the shaker and the test specimen, connected to the test specimen. It is important that the interface of the load transducer and the specimen limits/prohibits relative motion between the two, so as to not introduce a difference between the measured and actual structural excitation force. In mounting the load transducer to a test specimen by means of the attachment of an additional structure, at least one degree of freedom is essentially introduced in between the load cell and the test specimen.

The transmissibility of the system shown in Figure 6 is defined as the ratio of the transmitted force or amplitude to that of the excitation force or amplitude **[11]**, or:

$$TR = \left|\frac{X}{Y}\right| = \sqrt{\frac{1+(2\zeta\omega/\omega_n)^2}{[1-(\omega/\omega_n)^2]^2+[2\zeta\omega/\omega_n]^2}} \qquad \textbf{(8)}$$

The phase is given as:

$$\tan\psi = \frac{2\zeta\dfrac{\omega}{\omega_n}}{1-(\dfrac{\omega}{\omega_n})^2} \qquad \textbf{(9)}$$

When damping is considered to be negligible, as it is assumed to be in this case, the magnitude equation (8) reduces to:

$$TR = \left|\frac{X}{Y}\right| = \sqrt{\frac{1}{[1-(\omega/\omega_n)^2]^2}} \qquad \textbf{(10)}$$

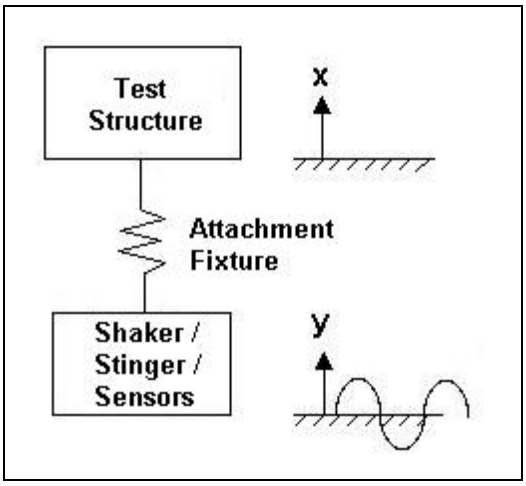

Figure 6. Coupled System

Ideally, the transmissibility ratio is unity over the test frequency range. This is equivalent to the test specimen being subjected to precisely the same excitation as the mounting fixture. In this application, however, this is not the case and the acceptable deviation from unity is a matter that must be addressed in each testing application.

The desired scope of applicability of the mounting fixture was discussed with lab faculty to be from 0 to 100 Hz. By limiting the transmissibility ratio to 1.1, the minimally acceptable frequency ratio is around 0.2, as shown in Figure 7. This indicates the minimum natural frequency of the mounting fixture should be approximately 500 Hz.

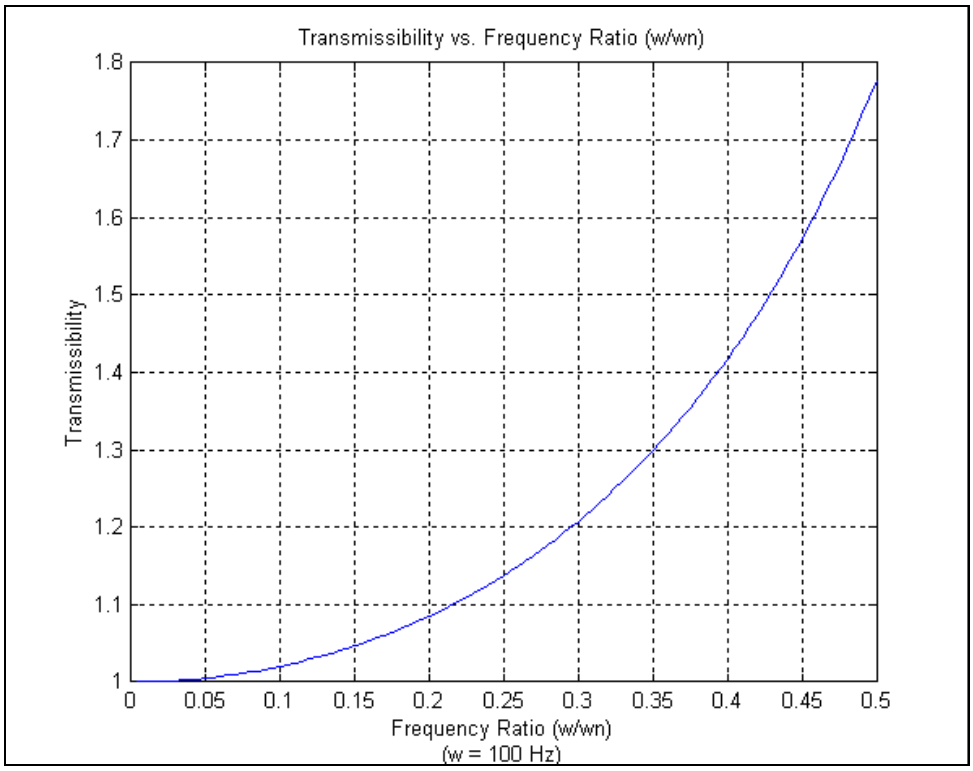

Figure 7. Transmissibility vs. Frequency Ratio

In addition to the transmissibility concern, the concept of "mass-loading" must be addressed. The addition of any mass to a structure will change its dynamic characteristics and in turn, will bias the measurements quantifying these dynamics. The addition of sensors to a test specimen introduces mass to the system being measured, which can introduce errors in determining the true natural frequencies of a system and quantifying its dynamic characteristics. The easiest way to avoid the introduction of these errors is to diminish the amount of mass added to the system being measured, and is

accomplished by using the lightest transducers and testing equipment possible [**12**]. With the need for lightweight testing equipment established, the mass of the attachment fixture becomes paramount.

Chapter 3 - Design Optimality

The theory of design optimization in a mechanical engineering perspective is well developed in texts including **[1]**, **[2],** and **[4]**. Numerical optimization in a more broad sense is well developed in texts including Wilde and Beightler **[13]** and Gottfried **[14]**. These references offer a wealth of information on the subject and should be consulted for an in-depth understanding of optimization, as only the critical foundations are reviewed here.

A standard, single objective optimization can be formulated by:

$$\text{minimize } f(\mathbf{x})$$

subject to:

$$\begin{aligned} g_1(\mathbf{x}) &\le 0 \\ &\vdots \\ g_m(\mathbf{x}) &\le 0 \\ h_1(\mathbf{x}) &= 0 \\ &\vdots \\ h_p(\mathbf{x}) &= 0 \end{aligned} \qquad \textbf{(11)}$$

Where $f(\mathbf{x})$ is the scalar valued objective function to be minimized and $\mathbf{x} \in R^n$ is defined as the design vector. The objective function $f(\mathbf{x})$ is subject to $g_1, \ldots, g_m$ scalar-valued inequality constraints and $h_1, \ldots, h_p$ scalar valued equality constraints, which bound the feasible design space. The design vector contains all of the modifiable parameters of the system. The point $\mathbf{x}^*$ is said to be feasible if and only if each of the equality and inequality constraints **(11)** are satisfied. The point $\mathbf{x}^*$ is said to be a local minimum if it is both feasible and if $f(\mathbf{x}^*) \leq f(\mathbf{x})$ within a particular region near $\mathbf{x}^*$. The point $\mathbf{x}^*$ is said to be a global minimum if the is both feasible and if $f(\mathbf{x}^*) \leq f(\mathbf{x})$ for all possible **x.**

3.1 Design Variable Formulation

The general form of the attachment fixture is shown in Figure 8.

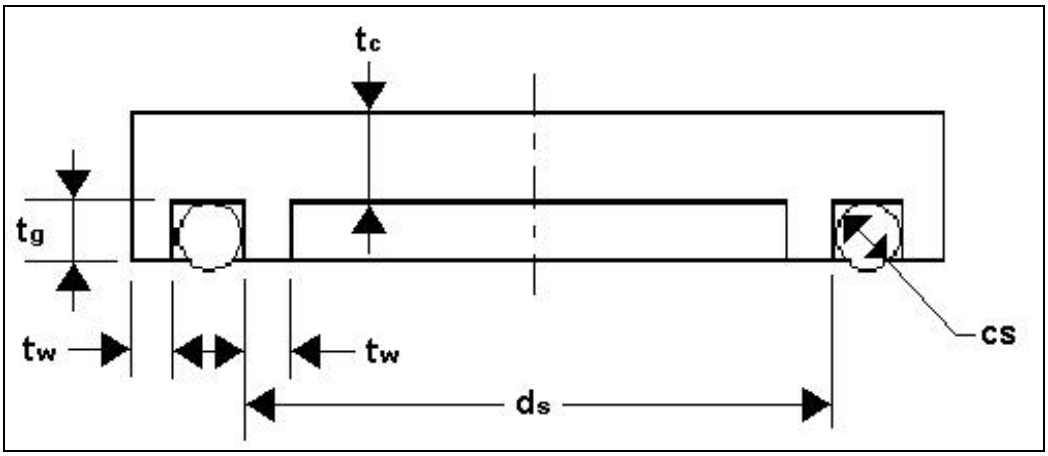

Figure 8. General form of Attachment Fixture

The design vector, **x**, is given as:

$$\mathbf{x} = (t_c, t_w, t_g, d_s, cs) \qquad (12)$$

Or:

$$\mathbf{x} = (x_1, x_2, x_3, x_4, x_5) \qquad (13)$$

Where:

$$x_1 = t_c$$

$$x_2 = t_w$$

$$x_3 = t_g$$

$$x_4 = d_s$$

$$x_5 = cs \qquad \textbf{(14)}$$

3.2 Constraint Formulation

The design of the attachment fixture is governed by the following inequality constraints, which are stated in the standard form as set forth by **(11)**:

Minimum natural frequency constraint:

$$f_n > 500 \text{ Hz} \qquad \textbf{(15)}$$

Where the cup is modeled as a clamped circular plate:

$$f_n = \frac{\lambda^2}{2\pi r^2}\sqrt{\frac{Et^2}{12\rho(1-\upsilon^2)}};\lambda^2 = 4\sqrt{\frac{\rho t \pi r^2}{M}} \qquad \textbf{(16)}$$

Where ρ is the material density; E is the elastic modulus of the material; t is the thickness of the clamped plate; r is the radius of the clamped plate; M is the associated point mass on the plate; and υ is Poisson's ratio for the plate material. The above equation is applicable by modeling the system as a clamped circular plate with a point mass located in the center **[15]**. The point mass includes the mass of the load cell, the stinger rod and mounting hardware, and the mass of the armature of the shaker. The frequency of 500 (Hz) follows from the discussion in the Definitions and Assumptions section regarding the transmissibility of the coupled system shown in Figure 7.

Minimum separation force constraint:

$$F_r \geq 30 \text{ lb } (135 \text{ N}) \qquad \textbf{(17)}$$

Where:

$$F_r = \pi \left(\frac{d_s + cs}{2}\right)^2 P_{vac} - c_{seal}\ \pi (d_s + cs) \qquad \textbf{(18)}$$

F_r is the force needed to separate the fixture from the test specimen, P_{vac} is the attainable vacuum, and c_{seal} is the seal compressive load per linear inch of seal. The force, F_r, is the resultant of the vacuum acting on the sealing area and the compressive load needed to compress the seal to the point to where the cup contacts the test specimen. The load value of 30 lb originates from the performance of the MB Dynamics Modal 50-A shaker, one of the shakers regularly used by the UC SDRL to perform modal analyses. The shakers have a maximum output of 25 lb peak during excitation without user supplied forced-air cooling **[16]**. Five pounds were arbitrarily added to the maximum output of 25 lb as a safety factor to ensure proper function of the attachment system at peak shaker output. The variable P_{vac} represents the maximum attainable vacuum and c_{seal} represents the seal compressive load per unit length of seal circumference.

Maximum radial stress constraint:

$$\sigma_r \leq 10 \text{ ksi } (68.9 \text{ MPa}) \qquad \textbf{(19)}$$

Where:

$$\sigma_r = \frac{6M_r}{t^2};\ M_r = 0.0796\ P \qquad \textbf{(20)}$$

The radial stress, σ_r, is calculated by modeling the fixture as a clamped circular plate with

an axial load applied at the center, which is the maximum stress incurred by an axis-symmetric plate in bending **[17]**. P represents the peak axial load, or F_a in this application.

Thin wall constraints:

$$t_w \geq 0.0625 \text{ in } (0.0016 \text{ m}) \qquad \textbf{(21)}$$

$$t_c \geq 0.0312 \text{ in } (0.0008 \text{ m}) \qquad \textbf{(22)}$$

The thin wall constraints ensure the manufacturability of the fixture and are chosen rather arbitrarily. Thinner wall thicknesses could lead to deflection during fabrication, resulting in an inability to produce needed surface finishes and to properly clamp the work piece during manufacture. The values chosen are purely based on the author's experience in a manufacturing setting.

Maximum seal compression constraint:

$$\text{Comp}_{max} = \frac{cs - t_g}{cs} < 40\% \qquad \textbf{(23)}$$

The maximum allowable compression of the seal is limited to 40% to ensure the seal is not over-compressed, leading to "compression set" or plastic deformation. Plastic deformation of the seal inhibits the ability of the fixture to adhere to curved surfaces and causes degradation of the seal's performance **[10]**.

Minimum seal compression constraint:

$$\text{Comp}_{min} = \frac{cs - t_g - h}{cs} > 5\% \qquad \textbf{(24)}$$

The minimum allowable seal compression constraint ensures the seal remains compressed at least 5% of its undeflected cross-sectional diameter when mounted in to a curved surface, as described as the curved mounting condition given in the Definitions and Assumptions section.

Minimum seal deflection constraint:

$$Comp_{min} * cs \geq 0.007 \text{ in } (1.7 \times 10^{-4} \text{ m}) \quad \textbf{(25)}$$

The minimum recommended deflection, regardless of cross-sectional diameter, is 0.007 in. Repeated use at extremely small deflections causes plastic deformation, possibly in the functional range of the design **[10]**. When taken into consideration with the minimum compression constraint **(25)**, it can be reduced to:

$$0.05 * cs \geq 0.007 \text{ in } (1.7 \times 10^{-4} \text{ m}) \quad \textbf{(26)}$$

Converting the above to the standard form set forth in the Design Optimality section and to SI units yields:

$$g_1(x) = 500\text{Hz} - \frac{4\sqrt{\frac{\rho_{cup} t_c \pi \left(\frac{ds}{2} - t_w\right)^2}{M_{armature,stinger}}}}{2\pi\left(\frac{ds}{2} - t_w\right)^2} \sqrt{\frac{E_{cup} t_c^{\,2}}{12\rho_{cup}(1-\upsilon_{cup}^{\,2})}} \leq 0 \quad \textbf{(27)}$$

$$g_2(x) = 135\text{N} - \pi\left(\frac{d_s + cs}{2}\right)^2 P_{vac} - c_{seal}\pi(d_s + cs) \leq 0 \quad \textbf{(28)}$$

$$g_3(x) = \frac{6 * 0.0796\, F_a}{t_c^{\,2}} - 68.9\,\text{MPa} \leq 0 \quad \textbf{(29)}$$

$$g_4(\mathbf{x}) = 0.0016 \text{ m} - t_w \leq 0 \quad \textbf{(30)}$$

$$g_5(\mathbf{x}) = 0.0008 \text{ m} - t_c \leq 0 \quad \textbf{(31)}$$

$$g_6(x) = \frac{cs - t_g}{cs} - 0.4 \leq 0 \qquad \textbf{(32)}$$

$$g_7(x) = 0.05 - \frac{cs - t_g - h}{cs} \leq 0 \qquad \textbf{(33)}$$

$$g_8(\mathbf{x}) = 0.00017\ m - 0.05 * cs \leq 0 \qquad \textbf{(34)}$$

3.3 Objective Function Formulation

With the desire to minimize the mass introduced to a modal test established Chapter 2, it becomes suitable for the mass of the attachment fixture to be used as the objective function of the design optimization. The mass of the fixture is modeled as the combined masses of the cup and the seal. Both are calculated by multiplying the corresponding material density by the computed volume of each body. The mass of the cup is given as:

$$mass_{cup} = \rho_{cup}\ \pi\left(\left(\frac{d_s}{2} + cs + t_w\right)^2 (t_g + t_c) - t_g\left(\frac{d_s}{2} + cs\right)^2 + t_g\left(\left(\frac{d_s}{2}\right)^2 - \left(\frac{d_s}{2} - t_w\right)^2\right)\right) \qquad \textbf{(35)}$$

The mass of the seal is given as:

$$mass_{seal} = \rho_{seal}\, 2\, \pi^2 \left(\frac{cs}{2}\right)^2 \left(\frac{d_s + cs}{2}\right) \qquad \textbf{(36)}$$

Combining the two yields the final form of the objective function:

$$f(x) = mass_{total} = \rho_{cup}\ \pi\left(\left(\frac{d_s}{2} + cs + t_w\right)^2 (t_g + t_c) - t_g\left(\frac{d_s}{2} + cs\right)^2 + t_g\left(\left(\frac{d_s}{2}\right)^2 - \left(\frac{d_s}{2} - t_w\right)^2\right)\right) + \rho_{seal}\, 2\, \pi^2 \left(\frac{cs}{2}\right)^2 \left(\frac{d_s + cs}{2}\right) \qquad \textbf{(37)}$$

Chapter 4 - Results

4.1 Optimization Model

The optimization problem given in the preceding sections was solved numerically by use of the gradient-based non-linear constrained minimization function "fmincon" of the Optimization Toolbox within MATLAB Version 6.1.

The optimization model of the attachment fixture consisted of a main executable, the objective function, the constraint function, and three other "utility" functions used to calculate three system parameters: a seal compression force calculation function, a maximum vacuum generated load, or F_{atm}, calculation function, and a chord height, h, calculation function. A graphical representation of the optimization model is shown in Figure 9.

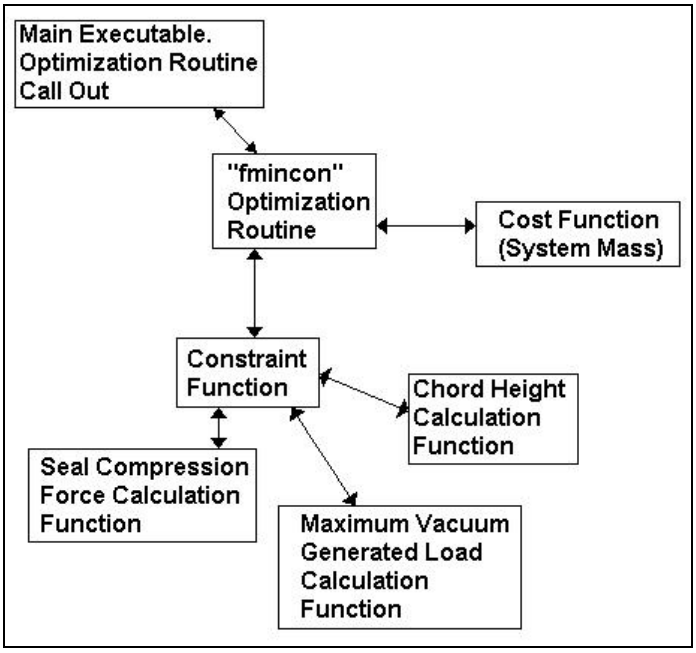

Figure 9. Optimization Model Diagram

The main executable function contains the pertinent physical and material constants of the design of the attachment fixture. Along with the constants, the upper and lower bounds of the design space and the optimization options are declared. The optimization function “fmincon” is called within the main executable.

The cost function, or objective function, is the total mass of the attachment fixture. The cost function calculates the total system mass when a given design vector is passed. The cost function is minimized by the optimization routine.

The constraint function contains all of the design constraints of the optimization problem. The constraint function, when a design vector is passed to it, outputs a scalar valued vector indicating the satisfaction of each of the design constraints. If the value of a constituent of the returned vector is negative, its corresponding constraint is said to be satisfied. If a constituent of the outputted vector is zero, it is implied that the corresponding constraint is active in the optimization, and hints at a potentially “optimal” point.

The three other “utility” functions calculate system parameters used by the constraint function when passed the design vector. The functions calculate the seal compressive force per linear inch of seal circumference, the chord height of the curved mounting condition seal-specimen interface, and the maximum attainable vacuum generated load.

4.2 Solution Considerations

The numerical solution of the design model proved to be sensitive to the initial design vector passed to the optimization routine, as the "optimal" solution of the model was noted to vary depending on the initial design vector. The variance in the "optimal" solution represented the solution routine converging to "locally" minimum solutions.

The tendency to converge to "locally" minimum solutions was averted by implementing incremental perturbations to constituents of the initial design vector, from the lower to the upper bounds of the design space. The optimization routine is run for each perturbation of the initial design vector, and each solution is stored in a solution matrix. The minimum or optimal solution can then be extracted by analyzing its corresponding objective function value. This method, while not guaranteeing convergence to the absolute global minimum solution, gives reasonable assurance of a near-globally minimal solution.

4.3 Optimized Solution

The optimized solution of the model is given as the following:

$$\mathbf{x}_{opt} = [0.0013 \quad 0.0016 \quad 0.0031 \quad 0.0420 \quad 0.0036] \text{ (m)}$$

or:

$$\mathbf{x}_{opt} = [0.051 \quad 0.063 \quad 0.122 \quad 1.654 \quad 0.142] \text{ (in)}$$

The above represents the obtained solution of the optimization with the globally minimal corresponding value of the cost function. The solution is shown in Figure 10.

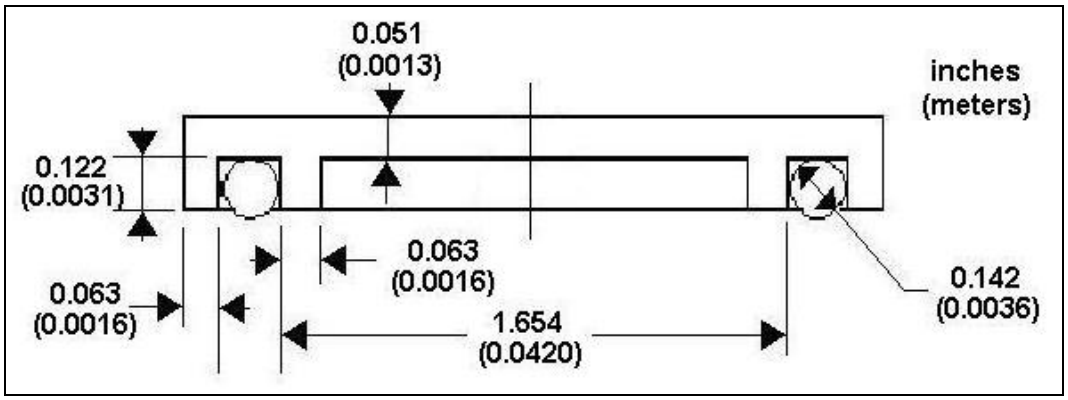

Figure 10. Optimized Solution of Attachment Fixture

4.4 Functional Constraint Sensitivity

Because the performance of the optimally designed system is highly dependent on the design constraints, it is of interest to analyze the sensitivity of the final "optimal" design to perturbations of the functional design constraints, namely, maximum applied load and minimum natural frequency. To analyze the model's sensitivity to constraint perturbation, the optimization model was solved for a range of maximum applied load and minimum natural frequency values. For the scope of this project, a simple "large" sensitivity analysis is performed by manually changing a constraint value and re-optimizing. A differential or "small" sensitivity analysis was not performed.

In the original design, the maximum applied load for the design constraint was set to be 30 lb, or 135 N, based on the output of current equipment used by the UC SDRL. If used in applications warranting lower peak applied force levels, the attachment fixture's design could be further optimized to take advantage of the less restrictive constraint. Likewise, if the attachment fixture was used in applications necessitating higher peak

applied loads, the peak applied load constraint must be adjusted accordingly. To analyze the optimization model's sensitivity to the maximum applied load, the optimization model was solved for peak load values from 100(N) to 165(N). The results of the analysis can be seen in Figure 11.

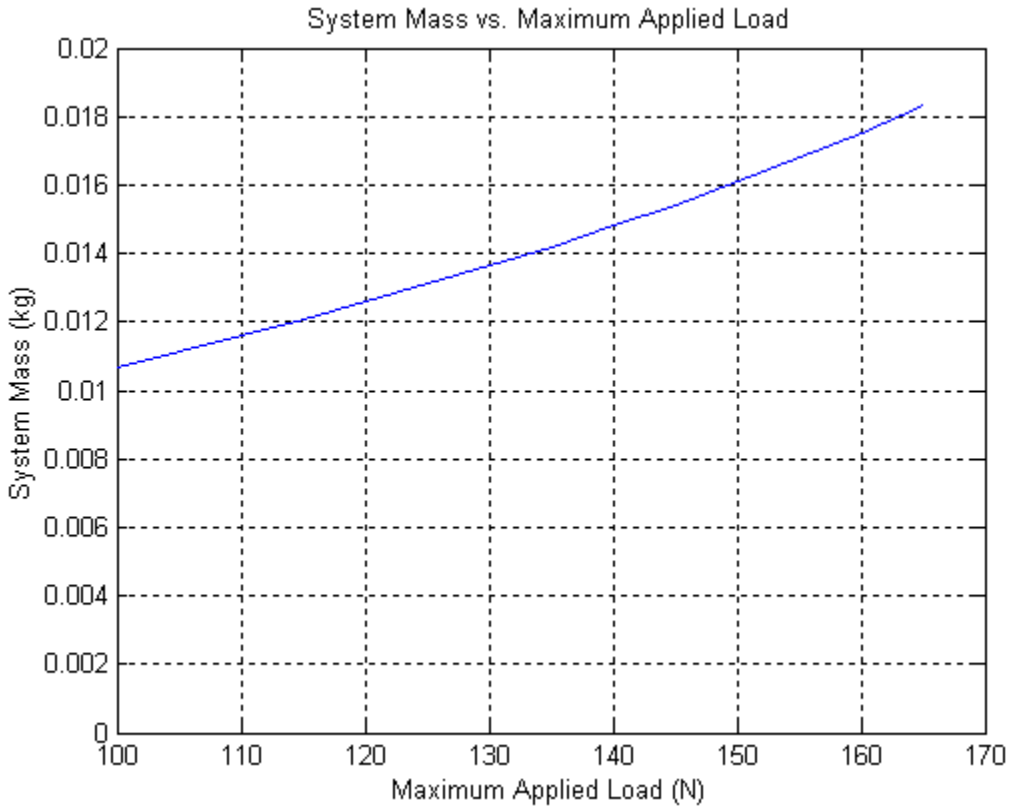

Figure 11. Design Sensitivity to Maximum Applied Load.

As evident in the above figure, a 10% increase in the maximum applied load constraint from the original value of 135 (N) results in an increase of approximately 10% in total mass.

The sensitivity analysis of the design to perturbations in the minimum natural frequency constraint is carried out similarly to that of the sensitivity analysis of the maximum applied load constraint. When the attachment is used in vibrations testing in lower

frequency ranges than that of the intended design range, the natural frequency constraint can be relaxed to the appropriate level. Likewise, when used in testing applications in higher frequency ranges, the natural frequency constraint must be adjusted to reflect the change. To analyze the sensitivity of the design to the minimum natural frequency constraint, the optimization model was solved for the frequency range of 250 (Hz) to 750 (Hz). The results of the analysis can be seen in Figure 12.

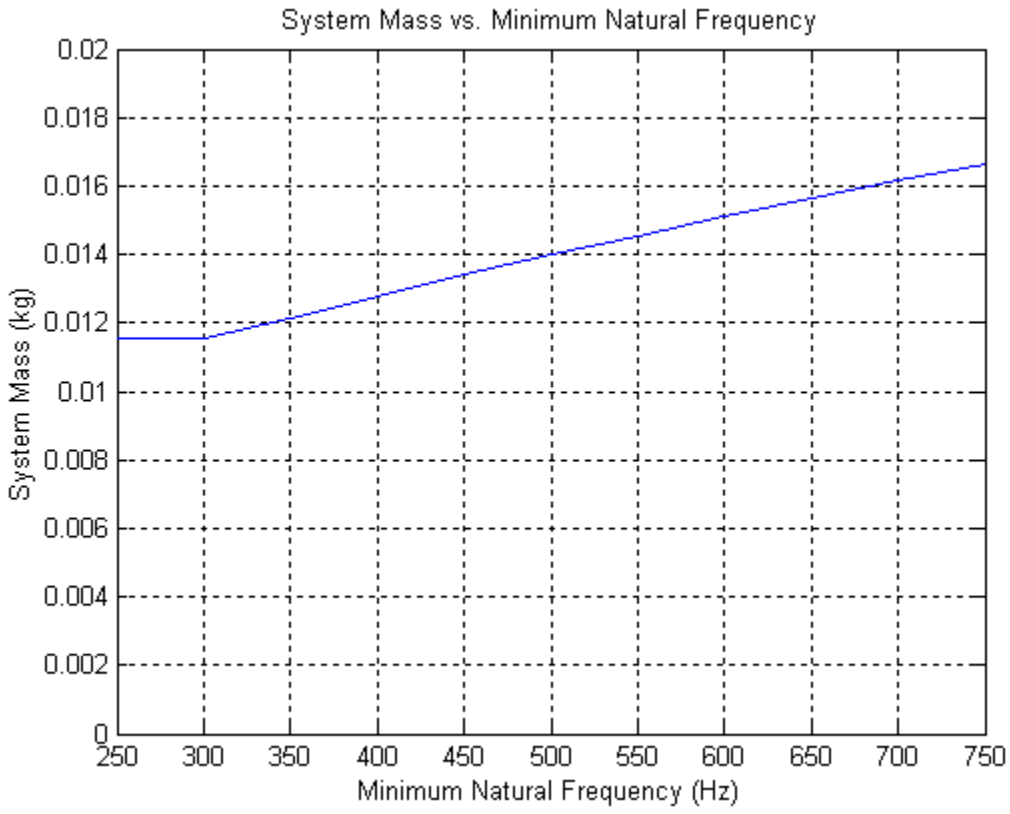

Figure 12. Design Sensitivity to Minimum Natural Frequency

As evident in Figure 12, a 10% increase in the minimum natural frequency of the attachment fixture from the original value of 500 (Hz) results in an increase of approximately 5% in total mass. A notable point shown in Figure 12 is the sensitivity of the design to the minimum natural frequency range of 250-300 (Hz). Over this range, the

system mass does not change, indicating the minimum natural frequency constraint is no longer active.

4.5 Design Adjustments for Fabrication

To avoid unnecessary manufacturing cost and effort, the design of the attachment fixture must be slightly adjusted for manufacture from its "optimal" form. These modifications must include geometric allowances for threaded portions for connection to a shaker and for the attachment of a barbed vacuum fitting. Along with allowances for threaded portions, the seal must be adjusted from the "optimal" value to correspond to readily available industry standard sizes. If so desired, a custom seal could be made for the device and the seal size would not need to be adjusted, but the scope of this project does not warrant the expense.

In the adjustment of the optimal solution to accommodate a standard seal size, consideration must be given to all constituents of the design vector so as to ensure a constraint violation is not caused by the design modification. The standard seal closest to the "optimal" design while satisfying the design and performance constraints has the following dimensions:

	Seal I.D. x(4)	Seal Cross Section x(5)
"Optimal" Design	1.653 (in)	0.142 (in)
Modified Design	1.750 (in)	0.139 (in)

Table 2. Comparison of "Optimal" and Modified Seal Size

When the design variables corresponding to seal size are adjusted to correspond to industry standard seal sizes, other design variables must be adjusted accordingly to avoid constraint violation. By adjusting the bounds of design vector in the optimization model, the design can be re-optimized while holding the design variables corresponding to seal size at their respective adjusted values. The result of the secondary optimization is given in Table 3.

Design Variable	x(1) t_c	x(2) t_w	x(3) t_g	x(4) d_s	x(5) cs	f(**x**) (mass)
Original Optimization	0.051 (in) 0.0013 (m)	0.063 (in) 0.0016 (m)	0.122 (in) 0.0031 (m)	1.654 (in) 0.0420 (m)	0.142 (in) 0.0036 (m)	0.0309 (lbm) 0.0140 (kg)
Secondary Optimization	0.055 (in) 0.0014 (m)	0.063 (in) 0.0016 (m)	0.115 (in) 0.0029 (m)	1.750 (in) 0.0445 (m)	0.139 (in) 0.0035 (m)	0.0337 (lbm) 0.0153 (kg)

Table 3. Comparison of Original and Secondary Optimizations

The adjusted design of the attachment fixture is seen in Figure 13. While the modification of the design does result in a solution considered "inferior" in terms of optimization, the effect of the modification is only a slightly more massive design. The adjustment of the "optimal" design vector causes an increase in mass of approximately 0.0013 (kg) or 10%.

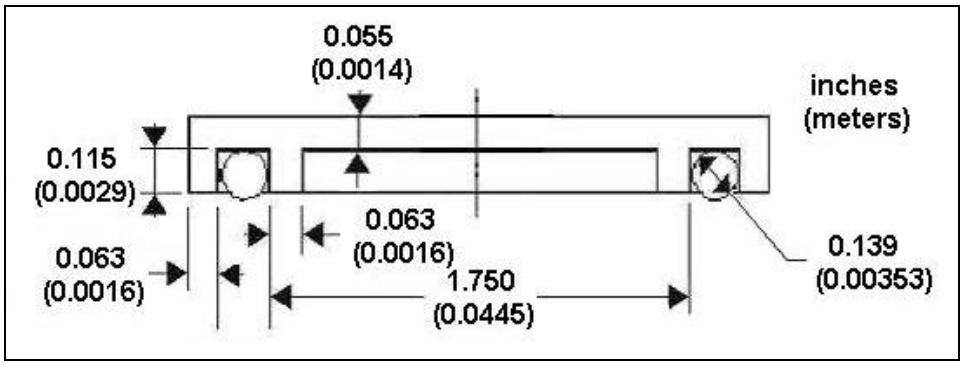

Figure 13. Design Adjusted for Standard Seal

The general design must also be modified to accommodate threaded attachment. Typically in shaker-excited vibrations testing, a long thin rod, or "stinger" connects the

exciter to a test specimen. The rod is typically attached by a collet-style clamp at the exciter end and by means of machine threads at the load cell/specimen end. To facilitate attachment of the load cell to the fixture, a cylindrical boss is added to the center of the design to allow for a larger threaded portion for greater thread engagement. In Figure 14, the adjusted form of the attachment fixture is shown.

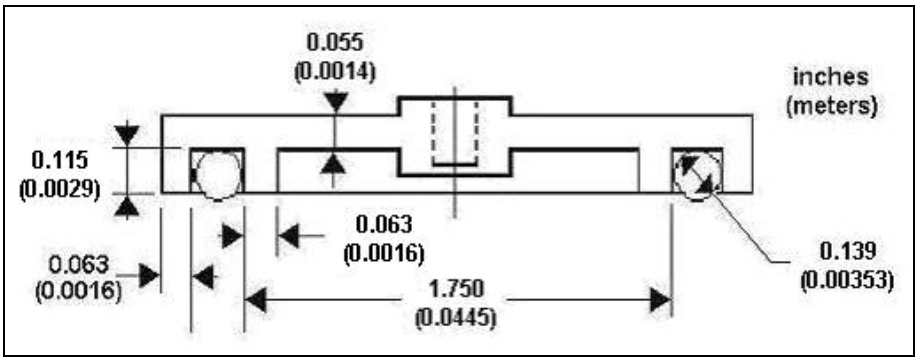

Figure 14. Adjusted Fixture Geometry for Threaded Attachment

4.6 System Performance

The design optimization provided an attachment fixture with a significantly reduced mass. A comparison is given in Table 4. The numerical optimization produces a design with 66% less mass than the existing design.

Design	Mass
Pre-Optimization	.057 (kg) *est.
"Optimal" Design	.019 (kg)

*The mass of the existing design was estimated by determining its volume by extracting geometry from pictures taken of the existing device and modeling in a solid modeling package.

Table 4. Comparison of Mass of the Two Designs

Chapter 5 - Experimental Evaluation

The suitability of the attachment fixture to perform vibrations experiments can be gauged by measuring the dynamic characteristics of a prototype fabricated to the specifications of the optimized design. As set forth in the preceding sections, the design of the fixture should avoid resonant frequencies near the intended testing frequency band.

The optimized design of the attachment fixture was functionally evaluated by performing a simple driving point frequency response measurement of a large rigid structure connected to a shaker by the attachment fixture. This is accomplished by taking force and acceleration measurements at the point of excitation by means of an impedance head sensor. The measurement was carried out for two shaker-structure attachment conditions, first by directly attaching the shaker to the structure by means of the stinger rod threaded into a threaded hole in the structure, second, by means of pneumatic attachment via the optimized attachment fixture.

The direct connection of the shaker to the structure by means of threaded connection can be said to exhibit the level of performance the pneumatic attachment fixture would ideally emulate. In practice, however, the addition of an additional structure in between the shaker and the test specimen will have an effect on the measured dynamic characteristics of the test specimen. The applicable frequency range of attachment fixture in a test setting can be determined by analyzing the frequency response measurements at the excitation point of both shaker attachment conditions and making a relative performance comparison between the two. The applicable frequency range is dictated by

factors in each testing application, so the applicability must be determined for each individual test.

To obtain the frequency response measurement, an impedance head sensor was installed in between the stinger and the test specimen. The impedance head is a dual acting sensor, comprising of a load cell and an accelerometer, which allow for simultaneous force and acceleration measurement at the excitation point. The force and acceleration data was acquired with MIMO-VXI and subsequently analyzed with X-MODAL II to determine the frequency response performance of the system. Both MIMO-VXI and X-MODAL II are MATLAB based software packages developed by the UC-SDRL. The test setup is shown in Figure 15.

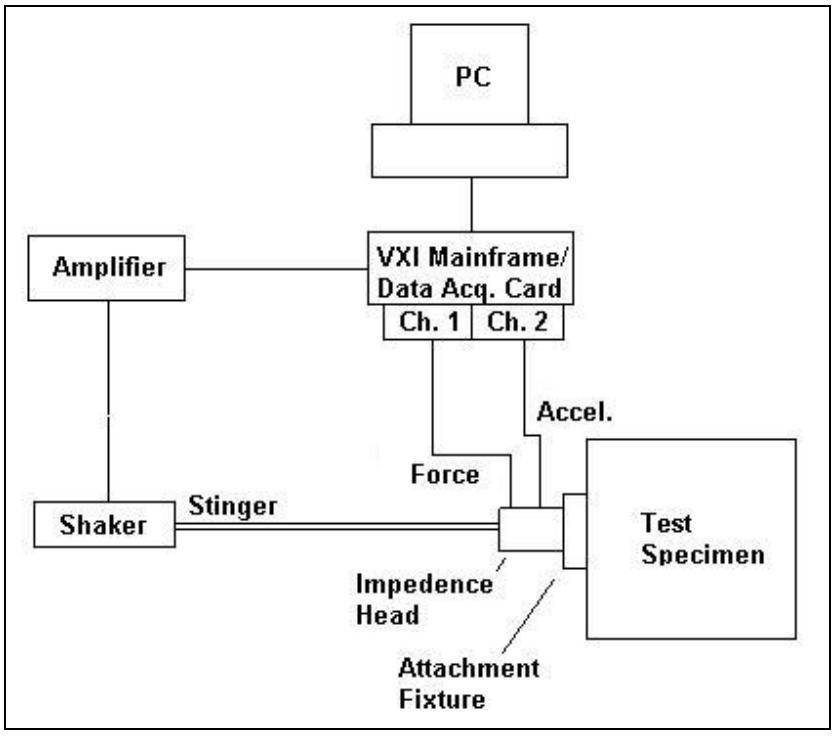

Figure 15. Test Setup Diagram

The test structure for the experiment was a large rectangular steel plate with a measured mass of 15.2 kg. The plate was suspended from a crane by shock cords and the shaker was suspended from an excitation stand as shown in Figure 16. The shaker and the test structure were connected via a 3/32" diameter stinger.

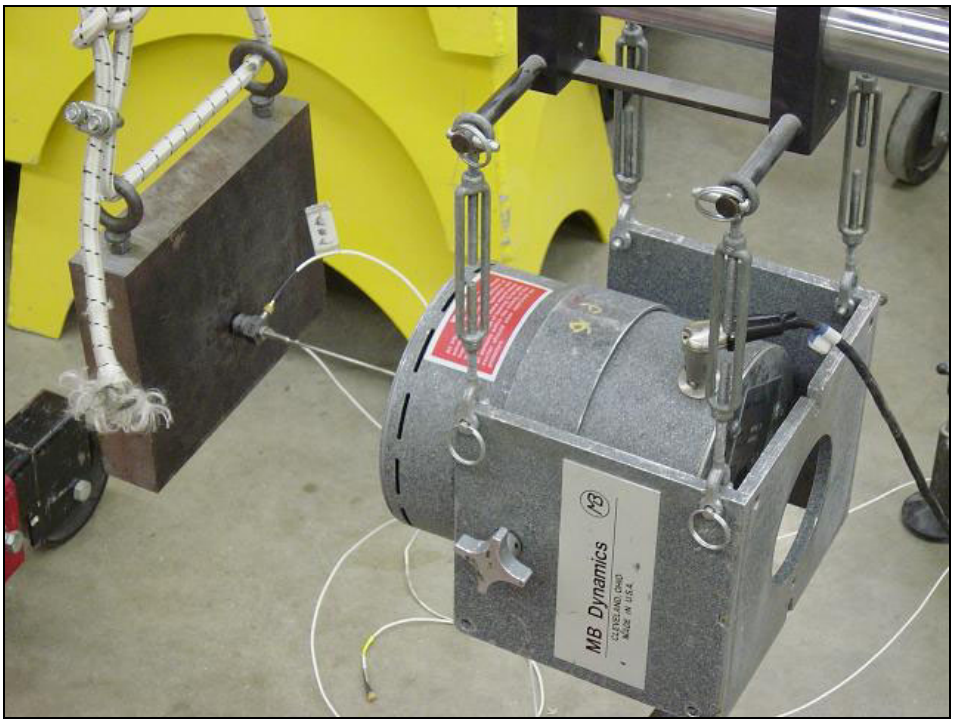

Figure 16. Test Structure and Shaker Setup

To establish a baseline of the characteristics of the test structure, the shaker was directly attached to the structure by means of a stinger and an impedance head, as shown above in Figure 16. The structure was given a random excitation from 0-1600 (Hz) and force and acceleration data at the excitation point was recorded and analyzed.

The obtained response of the system under the threaded attachment condition is shown in Figure 17. From the plot, it is apparent from the relative zero in data that the first resonant frequency of the attachment system is around 1300 (Hz).

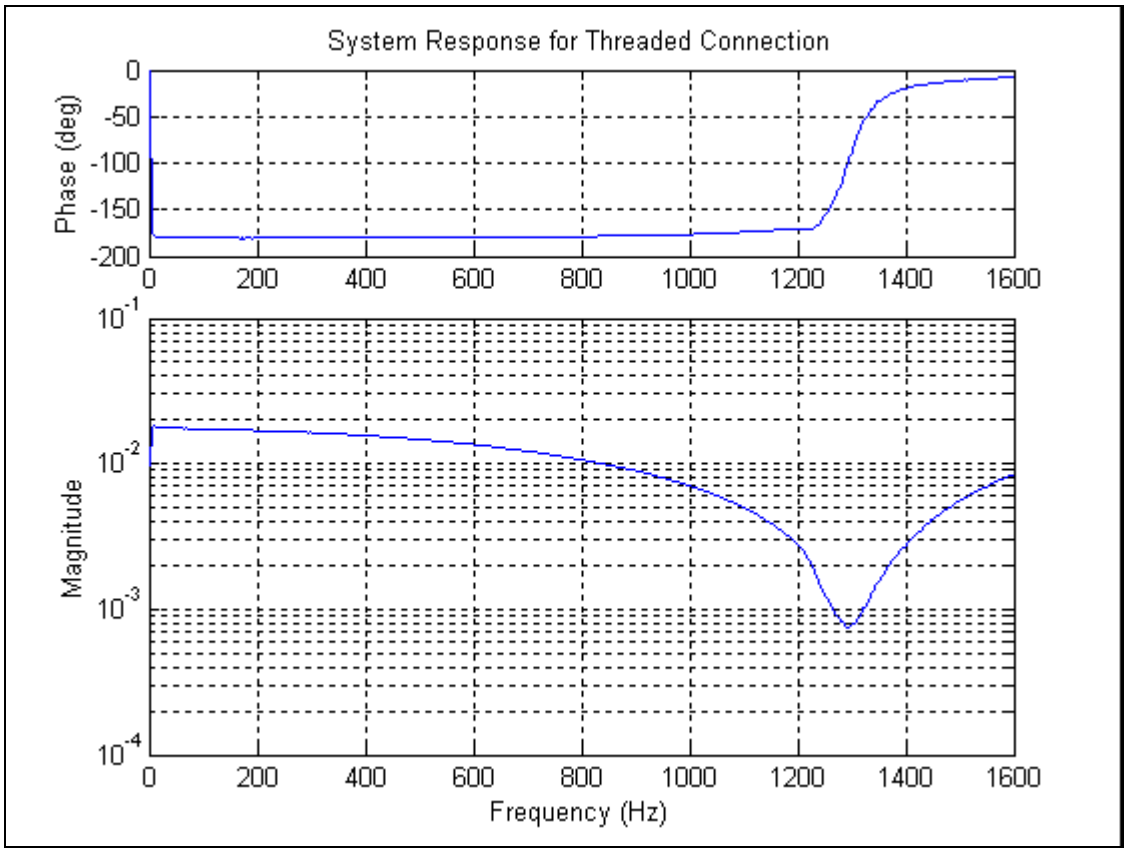

Figure 17. System Response for Threaded Connection

To evaluate the performance of the attachment fixture, the test was repeated for the same structure while using the attachment fixture to connect it to the shaker. All test parameters were held constant and care was taken to ensure the location of the attachment fixture was the same as the location of the threaded attachment point on the test structure. The setup is seen in Figure 18.

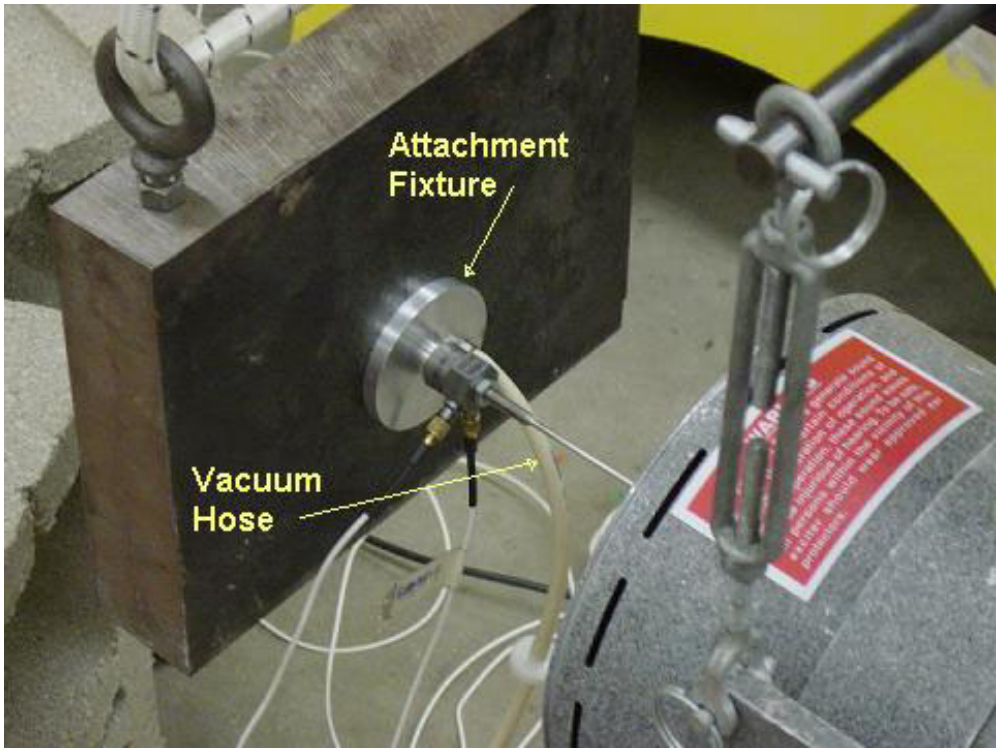

Figure 18. Pneumatic Attachment Fixture

The structure was given a random excitation from 0-1600 (Hz) and was analyzed as it was for the direct connection measurement. The obtained response of the system using the attachment fixture is shown in Figure 19**.** From the plot, it is apparent that the first resonant frequency of this attachment system is around 125 (Hz).

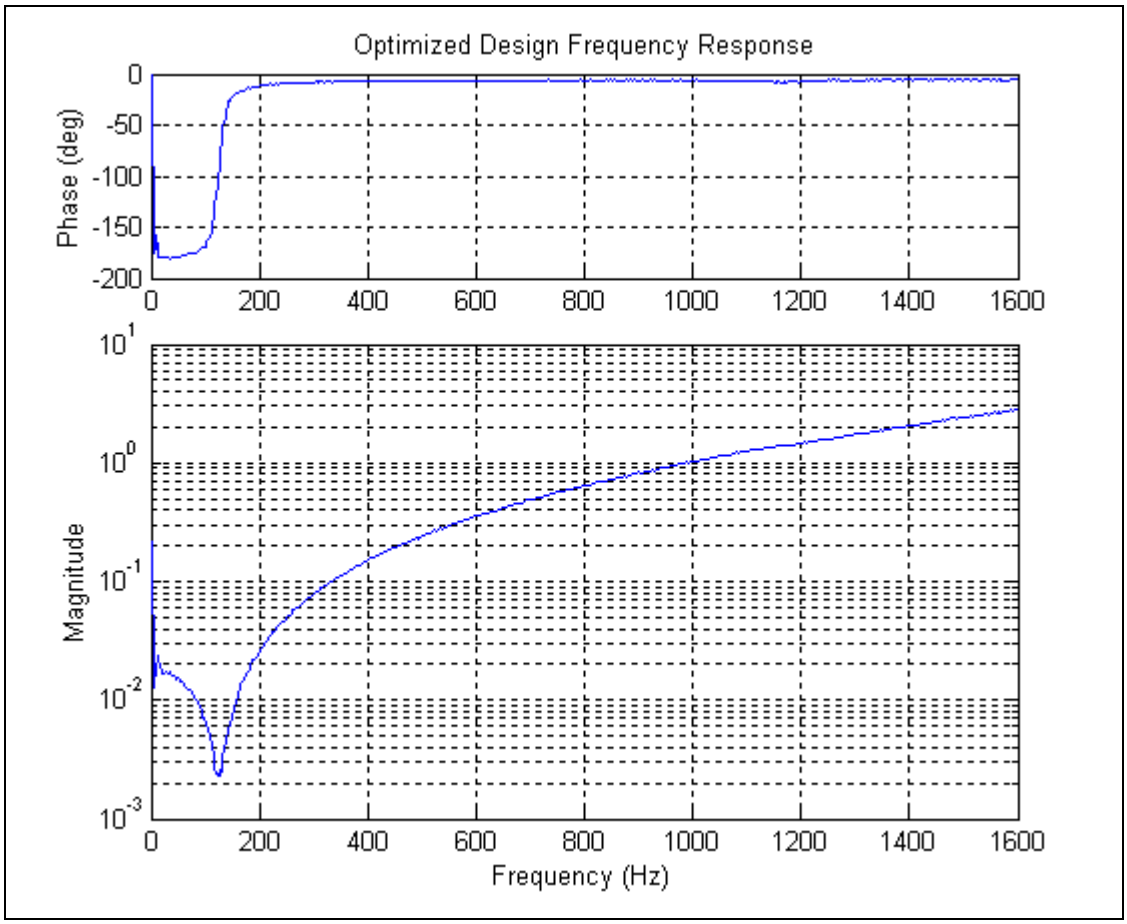

Figure 19. System Response with Attachment Fixture

A comparison of the frequency response of the two connection methods from 0-400 (Hz) is shown in Figure 20.

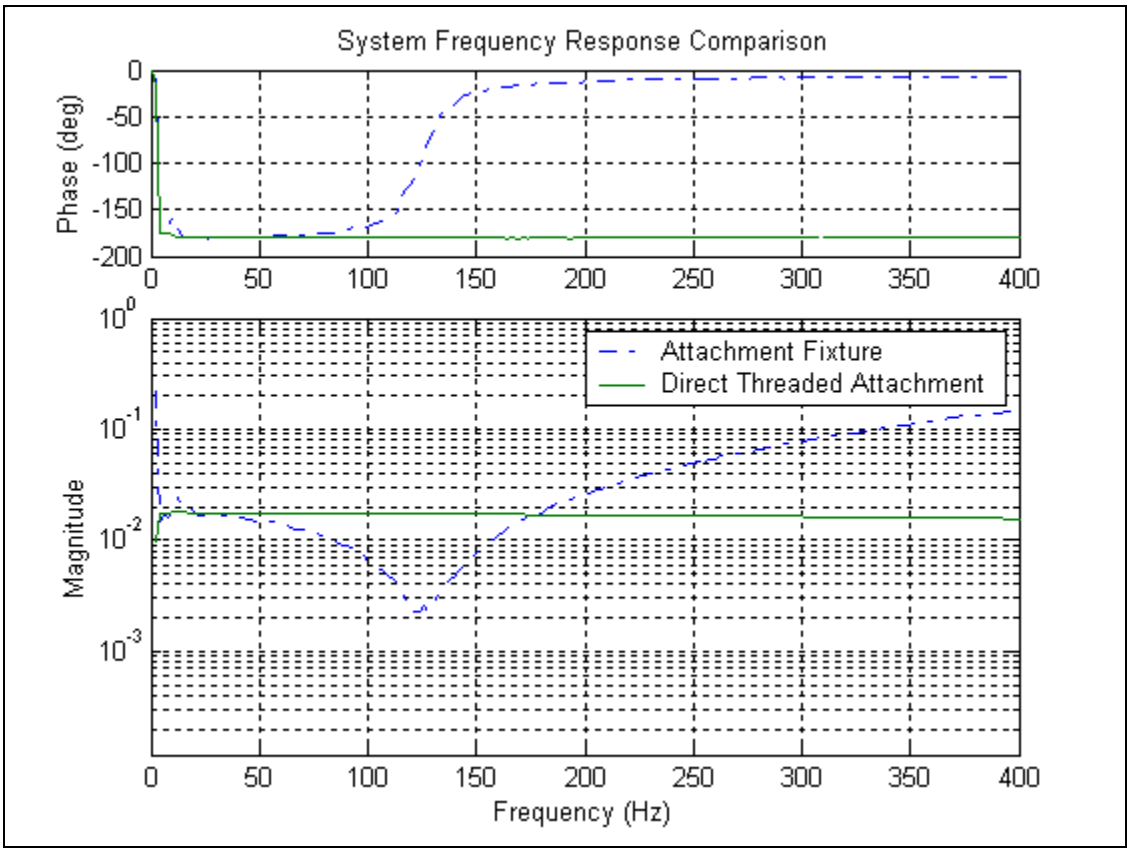

Figure 20. Comparison of Connection Method Performance

Chapter 6 – Redesign Analysis

The assumption of the cup being modeled as a clamped circular plated proved to be somewhat inadequate in predicting the first natural frequency of the design. The observed first natural frequency of the attachment fixture was approximately 120 (Hz). The target minimum first natural frequency in the design optimization was 500 (Hz), as put forth in the natural frequency constraint, Equation (16). This difference can be attributed to a number of factors.

First, the holes drilled in the fixture to accommodate treaded stinger attachment and the attachment of the vacuum hose become suspect of causing the decrease in natural frequency. The presence of the hole in the center of the fixture and the placement of a hole in the fixture for the vacuum fitting would result in a marginal loss in stiffness of the attachment fixture.

6.1 Increased Thickness

To determine if the thickness $\mathbf{x}_1$ could be increased to increase the natural frequency of the attachment fixture, a second prototype was fabricated with $\mathbf{x}_1$ doubled arbitrarily to 0.110 (in). All other design variables were held at the previous solution to ensure no other factors influenced the obtained results. The increase in thickness made a significant increase in natural frequency, from 125 (Hz) to 210 (Hz). A plot of the frequency response measurement is shown in Figure 21.

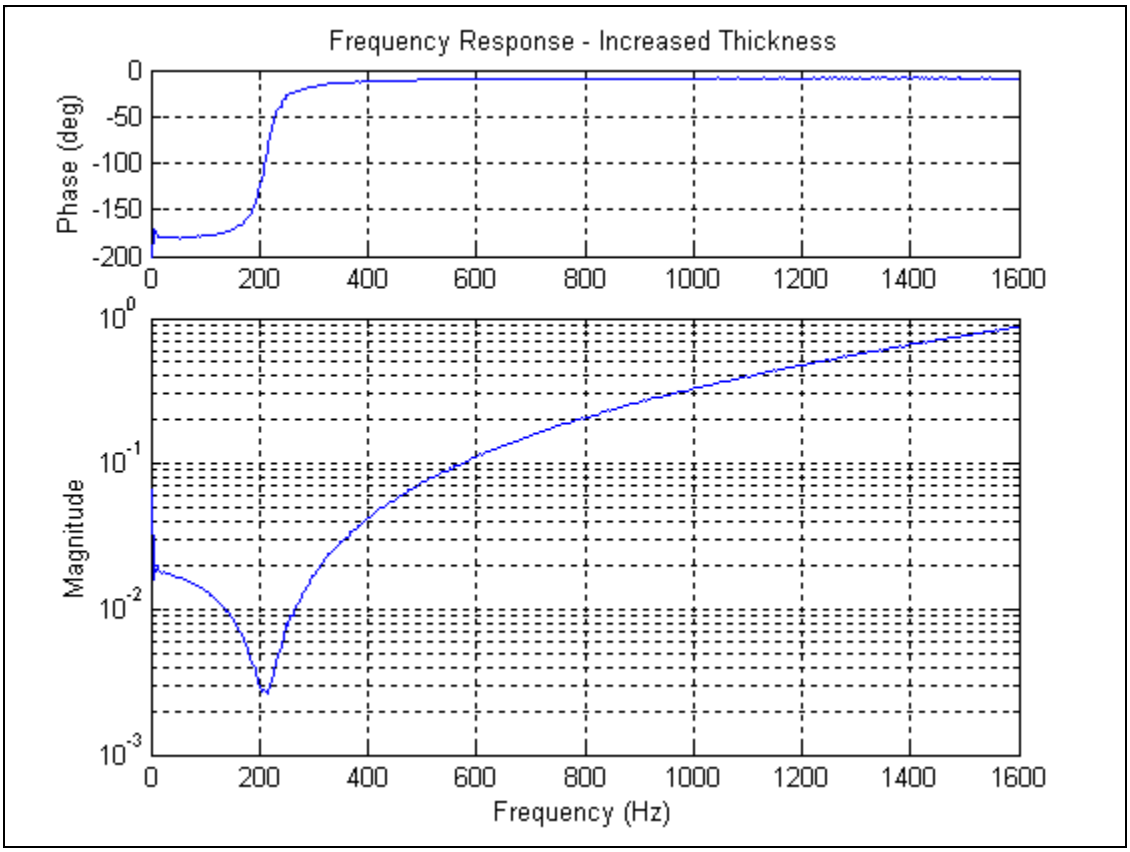

Figure 21. Frequency Response of Thickened Fixture

When compared, it is noted that the response of the fixture of increased thickness closely resembles the response of the threaded attachment of the shaker to the test structure for the frequency range of roughly 0-50 (Hz). A comparison of the two responses is shown in Figure 22.

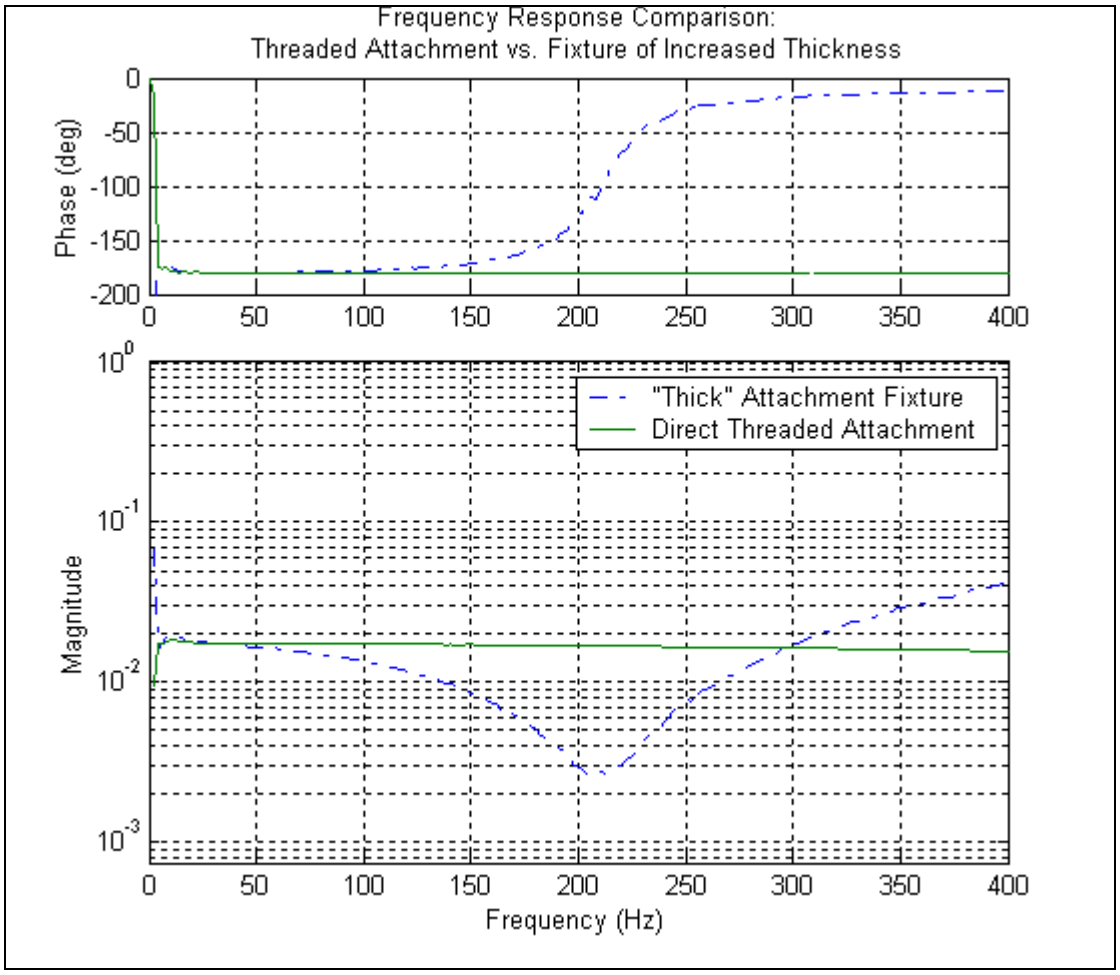

Figure 22. Response Comparison of Threaded Attachment and "Thick" Fixture

The increase in thickness of the fixture results in a mass to 0.029 (kg), or an increase of 0.010 (kg) or roughly 34%. The increased mass, however, is still well the "pre-optimization" mass of 0.057 (kg).

6.2 Adhesive Attachment

Secondly, the assumption of the plate being clamped can be inspected for validity. To determine if relative motion between the fixture and the test structure caused the low resonant frequency, the obtained frequency response measurement of the cup was compared to a frequency response measurement of the fixture glued to the test structure

with a cyanoacrylate adhesive. The use of a thin layer of cyanoacrylate adhesive ensures the fixture is fixed relative to the test structure at the fixture's base. When bonded to the fixture to the test structure, the first natural frequency of the system is measured to be approximately 140 (Hz). This is a slight increase from the earlier obtained value of 125 (Hz), but not close to the desired first natural frequency of 500 (Hz). This observed increase in frequency shows that the cup's mounting orientation imparts a notable effect on the fixture's first natural frequency. The results of the test are shown in Figure 23.

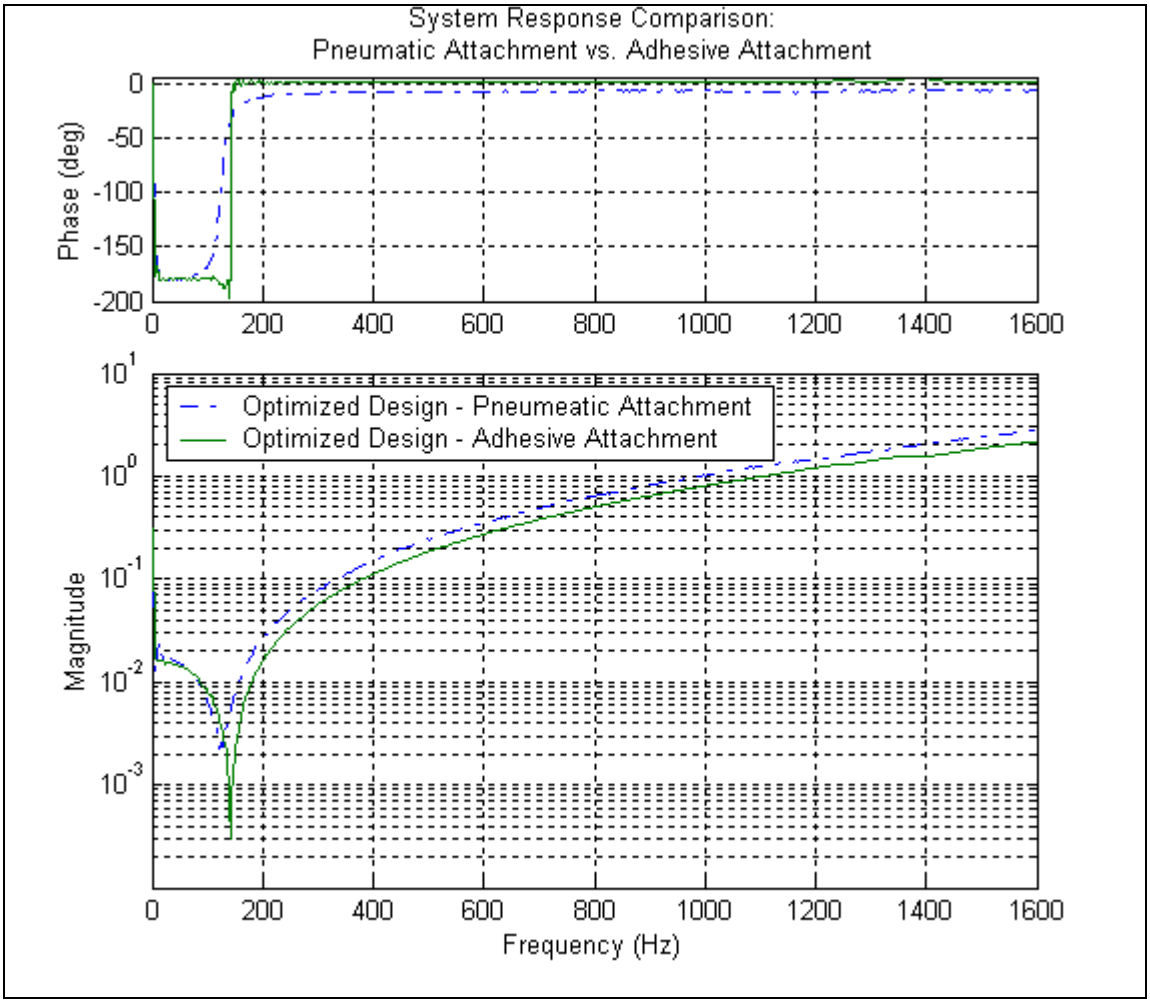

Figure 23. Comparison of Adhesive Attachment and Pneumatic Attachment

6.3 Finite Element Modeling

While the thickened attachment fixture yielded a more desirable result, the experimentally obtained frequency response of the attachment fixture still varies greatly from that of the desired result. To analyze the natural frequency of the attachment fixture in a configuration replicating that of its functional environment, a finite element model of the cup was generated and analyzed using ANSYS 6.1. A mass of 0.218 (kg) representing the armature mass in the optimization model was attached to the model of the cup to ensure an accurate result.

The finite element simulation was performed with the boundary condition of the mounting face of the cup, as shown in Figure 24, as being fixed, or, clamped to the test structure. This, to the author's knowledge, replicates the assumption made in the optimization model as closely as possible.

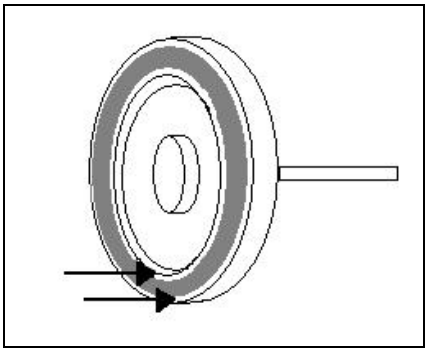

Figure 24. Mounting Surface of Attachment Fixture

The result from the finite element model, compared with the experimentally obtained natural frequency of the attachment fixture, is shown in Table 5.

Analysis	Result
Experimental	125 (Hz)
Finite Element	830 (Hz)

Table 5. Comparison of Experimental and Finite Element Results

As evidenced in the above table, the finite element model, which should closely approximate the actual solution, is far from the experimentally obtained result. With these findings, two possibilities are considered: An inaccurate natural frequency equation, or an inappropriately applied boundary condition in the optimization model.

6.4 Discussion

To investigate the source of the modeling inaccuracy, the analytical equation used to estimate the first natural frequency was inspected. The formulation of the optimization model states that the cup acts as a clamped circular plate with a point mass located in the center. A finite element model of a simple disc of dimensions corresponding to the adjusted optimal design was compared to the numerical result given by equation **(16)**. The finite element model utilized the same clamped boundary condition as the analytical equation **(16)**. Results for both the finite element model and the equation were calculated for varying masses from 0.025 (kg) to 0.25 (kg). The comparison is shown in Figure 25.

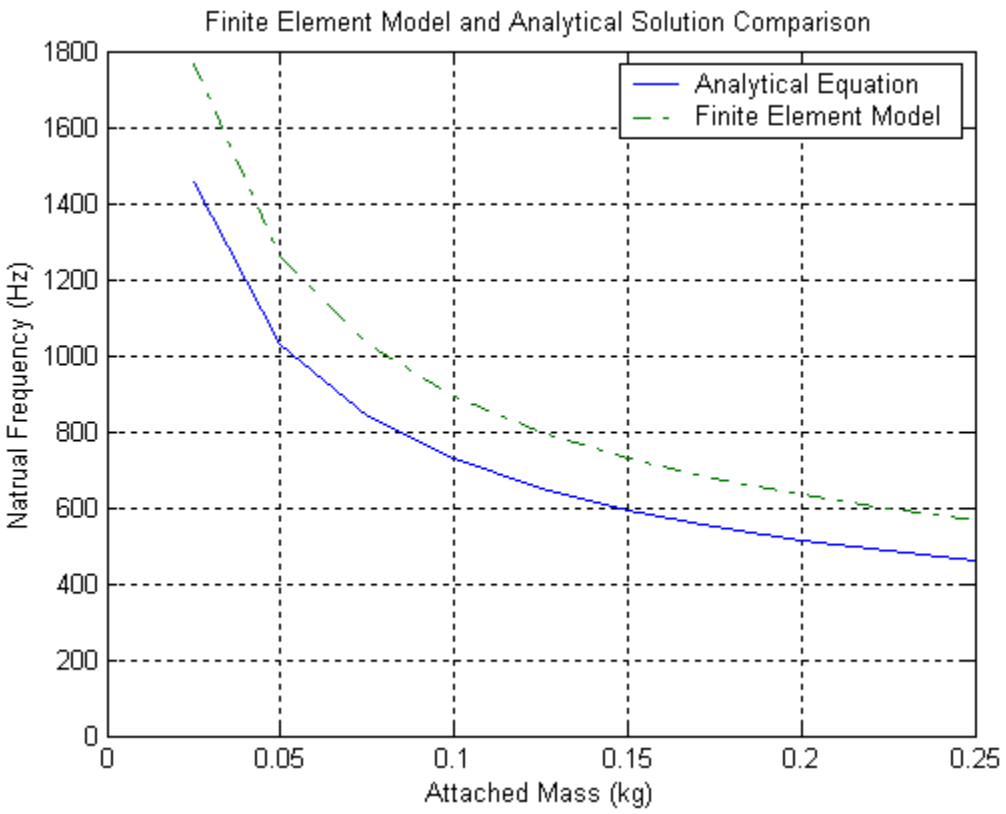

Figure 25. Finite Element Model and Analytical Solution Comparison

The comparison shown above in Figure 25 shows that the analytical expression yields a reasonably close result to that of the finite element model. With the verification of the natural frequency expression with the finite element model, the focus turns to the boundary condition assumed in the analytical model.

To investigate the effect of altering the assumed boundary condition of the fixture, a simply supported, or pinned, boundary condition is explored. The equation given for the first natural frequency of a simply supported circular plate with a point mass located in the center is given by: **[15]**

$$f_n = \frac{\frac{4}{(3+4\upsilon_{cup}+\upsilon_{cup}^2)}\sqrt{\frac{\rho_{cup} t_c \pi (\frac{ds}{2} - t_w)^2}{M_{armature,stinger}}}}{2\pi (\frac{ds}{2} - t_w)^2} \sqrt{\frac{E_{cup} t_c^2}{12\rho_{cup}(1-\upsilon_{cup}^2)}} \quad \textbf{(38)}$$

A comparison of the result obtained for the geometry of the adjusted optimal solution from the above expression and a finite element model of a simply supported disk of the same dimensions with a point mass located in the center is given in Figure 26.

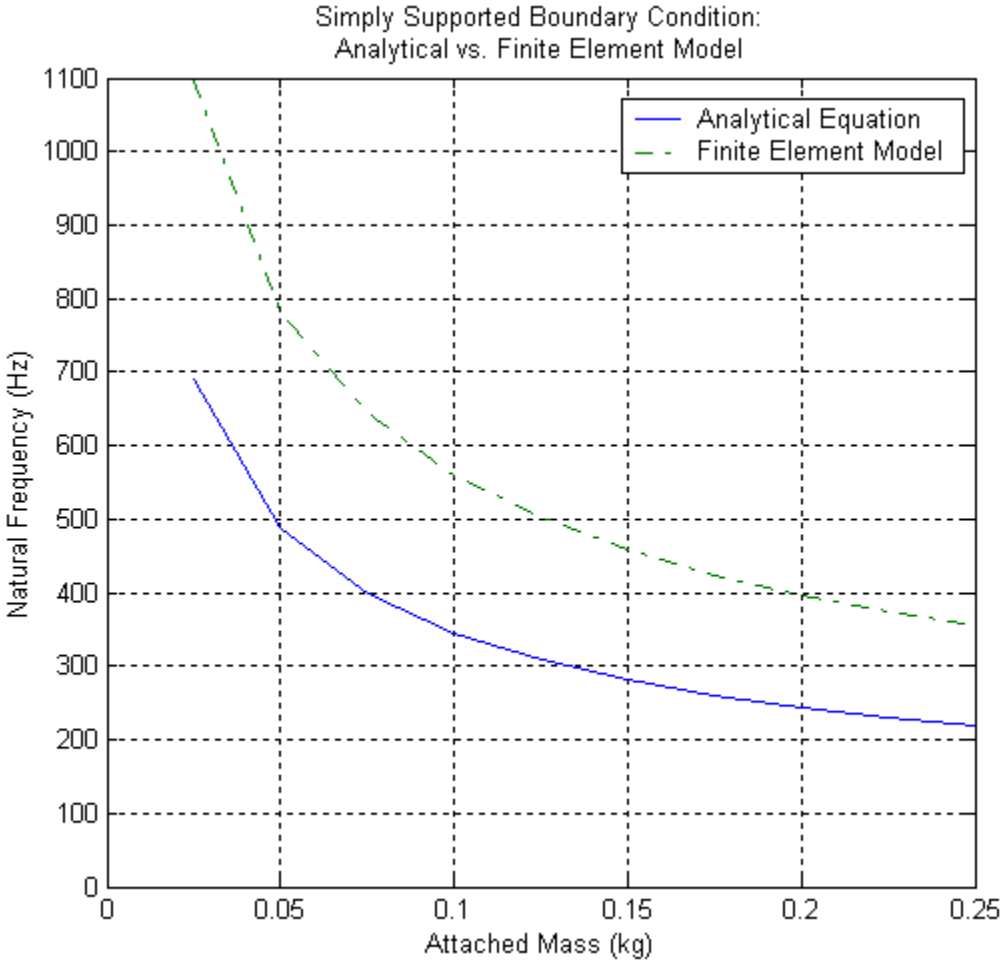

Figure 26. Comparison of Simply Supported Boundary Condition

The above figure gives a reasonable verification of the correlation of the analytical expression and the finite element model. An important observation is made that the

natural frequency of the two simply supported boundary condition solutions are much lower than those given by the solutions given by the clamped boundary condition.

With the difference of the calculated natural frequency established between the two boundary conditions, a finite element model of the design solution was analyzed with a simply supported boundary condition around the inside edge of the cup, as shown in Figure 27.

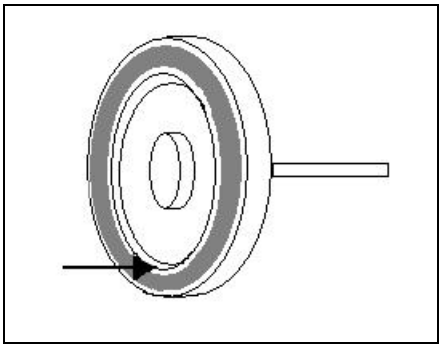

Figure 27. Simply Supported Boundary Condition Constraint Location

The result of the finite element model solution is shown below with the solutions obtained with the clamped boundary condition in Table 6.

Analysis	Result
Experimental	125 (Hz)
Finite Element (Clamped B.C.)	830 (Hz)
Finite Element (Simple Support B.C.)	684 (Hz)

Table 6. Solution Comparison with Different Boundary Conditions

While closer to the experimentally obtained value, the finite element model with a simply supported boundary condition still does not yield a natural frequency approximating the experimentally obtained value. With this established, it is the author's belief that the

cause of the lower than desired natural frequency is a combination of the fixture's modeled boundary condition and slight relative motion between the fixture and the specimen.

Chapter 7 - Conclusions

In this thesis a design optimization methodology was created for an attachment fixture to connect an electromagnetic shaker to a test specimen in vibrations testing. An optimization model of the attachment fixture was developed in MATLAB and this model was numerically optimized to minimize mass while meeting specified performance criteria. The numerical optimization produced a solution using a classical gradient-based algorithm. The initial result of the optimization was a 66% reduction in mass over the existing design, but the optimized solution failed to meet the minimum natural frequency criteria.

The attachment fixture offers an option of shaker attachment in low frequency vibrations testing such as automotive and aerospace applications. Surface damage due to shaker attachment is eliminated, as is the need to alter the test structure to enable the attachment of the shaker. The fixture offers a quick, easily adjusted method of attachment of a shaker to a test structure.

When the attachment device was functionally evaluated, it became apparent that the optimization model inadequately addressed the predicted natural frequency of the device. To investigate a possible solution to the insufficient dynamic performance of the design, a design variable, namely $\mathbf{x}_1$, was doubled from the optimized design. This resulted in a significant increase in the first natural frequency of the attachment fixture, but still not near the desired value of 500 (Hz).

To investigate the source of the difference between the modeled and the experimentally obtained natural frequency of the attachment fixture, a finite element model was developed and analyzed for different boundary conditions. The finite element analysis yielded higher values of natural frequency than those that were experimentally obtained. It is the author's opinion that the cause of the lower than desired natural frequency is a combination of the fixture's modeled boundary condition and slight relative motion between the fixture and the test structure.

The insufficient dynamic performance of the attachment fixture emphasizes the importance of an accurate model in design optimization. The accuracy of a numerically optimized solution is wholly dependent on the validity of a model. If the model of a system does not fully characterize its physical behavior, a numerically optimized solution is of little consequence, though can still provide trend and sensitivity information about the design. While numerical optimization is sensitive to modeling accuracy, the process provides engineers with an indispensable utility for design refinement in engineering endeavors, especially in systems with well-developed, accurate models.

Further Work

To further the refinement of the design of the attachment fixture, several options could be investigated. First, a parameterized finite element model could be interfaced with the design optimization. Starting with the optimized solution presented in this paper, a finite element analysis could be performed on the fixture to determine the first resonant frequency. With this known, perturbations could be given to each design variable

resulting in different design vectors to be analyzed in a finite element package to determine each design vector's first natural frequency. From these simulations, a model of the natural frequency of the attachment fixture could be constructed and implemented in the optimization model.

Secondly, the interface of the attachment fixture and the test structure could be analyzed to determine the validity of the assumption that the fixture remains stationary relative to the test structure in operation, so long as the minimum separation force constraint (18) is satisfied. When the fixture was bonded to the test structure with cyanoacrylate adhesive, a slight increase in natural frequency was noted. While bonding the fixture to the test structure did slightly improve its dynamic performance, it proved that the undesirably low resonant frequency was not exclusively due to relative motion between the fixture and test structure. Experiments could be performed to determine the actual behavior of the interface of the fixture and test structure, which would be a very noteworthy contribution to the modeling of the attachment fixture.

Lastly, because the fixture was designed to accommodate curved surface mounting, a performance evaluation of the attachment fixture could be performed on a test structure with a curved mounting surface. This experiment could determine the suitability of the system to attach a shaker to a curved surface such as certain portions of an automotive body or an aerospace structure. The effect of not having contact between the fixture and the test structure around the entire perimeter of the fixture could be analyzed. A possible problem with mounting to a curved surface being that the possibility of the fixture

rocking back and fourth on the point of contact, causing an unaccounted experimental inaccuracy.

References

[1] J. S. Arora, *Introduction to Optimal Design*, McGraw-Hill: New York, 1989.

[2] K. Otto and K. Wood, *Product Design: Techniques in Reverse Engineering and New Product Development*, Prentice Hall: Upper Saddle River, New Jersey, 2001.

[3] P. Y. Papalambros and D.J. Wilde, *Principles of Optimal Design: Modeling and Computation*, Cambridge University Press: Cambridge, UK, 1998.

[4] S. S. Rao, *Engineering Optimization: Theory and Practice*, Wiley: New York, 1996.

[5] D. F. Thompson, S. Gupta, and A. Shukla, "Tradeoff analysis in minimum volume design of multi-stage spur gear reduction units," *Mechanism and Machine Theory*, (35), pp. 609-627, 2000.

[6] J. Faiz and M. B. B. Sharifian, "Optimum design of a three phase squirrel-cage induction motor based on efficiency maximization," *Computers and Electrical Engineering*, (21), pp. 367-373, 1995.

[7] C. Good and J. McPhee, "Dynamics of mountain bicycles with rear suspensions: design optimization," *Sports Engineering*, (3), pp. 49-55, 2000.

[8] K. –H. Hwang, K. –W. Lee, and G. –J. Park, "Robust optimization of an automobile rearview mirror for vibration reduction," *Structural and Multidisciplinary Optimization*, (21), 300-308, 2001.

[9] A. E. Baumal, J.J. McPhee, and P.H. Calamai, "Application of genetic algorithms to the design optimization of an active vehicle suspension system," *Computer Methods in Applied Mechanics and Engineering*, (163), pp. 87-94, 1998.

[10] Parker Hannifin Corporation, *Parker O-Ring Handbook 2001 Edition*, Cleveland, Ohio, 2001.

[11] W. T. Thomson and M. D. Dahleh, *Theory of Vibration with Applications*, Prentice Hall: Upper Saddle River, New Jersey, 1998.

[12] O. Dossing, "Prediction of Transducer Mass-Loading Effects and Identification of Dynamic Mass," *Proceedings of the 9th International Modal Analysis Conference*, pp. 306-311, Florence, Italy, 1991.

[13] D. J. Wilde and C. S. Beightler, *Foundations of Optimization*, Prentice Hall: Englewood Cliffs, New Jersey, 1967.

[14] B.S. Gottfried and J. Weisman, *Introduction to Optimization Theory*, Prentice Hall: Englewood Cliffs, New Jersey, 1973.

[15] R. D. Blevins, *Formulas for Natural Frequency and Mode Shape*, Van Nostrand Reinhold Company: New York, 1979.

[16] MB Dynamics, Inc., *Modal 50A Vibration Exciter*, MB Dynamics, Inc., Cleveland, Ohio, 1990.

[17] R. D. Cook and W. C. Young, *Advanced Mechanics of Materials*, Prentice Hall: Upper Saddle River, New Jersey, 1999.

Appendix

MATLAB Scripts

Main Executable

```
%%%%%%%%%%%%%%%%%%%%%%%%%%%%%%%%%%%%%%%%%%%%%%%%%%%%%%%%%%%%%%%%%%%%%%%%%%%%%%%
% This script defines physical constants and design constants and performs the
% optimization for the design of the vacuum mount sensor fixture.  It varies
% starting value for the optimization routine to ensure local minima are
% eliminated from the optimized design vector

clear all

global rhocup rhoseal emodcup poiscup bendrad maxvac maxshak armmass x5ub
disp('-------------------------------------------------------------------------------');
disp('Vacuum cup optimization');
disp('-------------------------------------------------------------------------------');
tic;

% Determine number of intervals to split minimum and maximum bounds of design
% varibles for the initial design vector in the optimization routine
meshsize = 8;
%%%%%   Design vector bounds
x1lb = .0001;
x1ub = .01;

x2lb = .0001;
x2ub = .01;

x3lb = .0001;
x3ub = .01;

x4lb = .04444;
x4ub = .04446;
x4inc = (x4ub-x4lb)./meshsize;

x5lb = .00353;
x5ub = .00354;
x5inc = (x5ub-x5lb)./meshsize;

% Physical and design constants

rhocup = 2710;           % cup material density (kg / m^3)
rhoseal = 910;           % seal material density (kg / m^3)
emodcup = 71E9;          % elastic modulus of cup material (Pa)
poiscup = .33;           % poisson ratio for cup material
bendrad = .75;           % minimum radius of curvature of specimen (m)
maxvac = 93000;          % maximum attainable vacuum of vacuum pump (Pa)
armmass = .218;          % total mass of shaker armmature and stinger rod (kg)
maxshak = 135;           % Max shaker load (N)
```

```
%vecsize=size(x1lb:x1inc:x1ub);

% Declare options for optimization routine

options=optimset('DerivativeCheck','on','Display','off','GradConstr','off','GradObj',...
   'off','LargeScale','off','TolFun',1E-6,'MaxFunEvals',500,'TolCon',1E-6,'MaxSQPIter',180);

xlb = [x1lb x2lb x3lb x4lb x5lb];
xub = [x1ub x2ub x3ub x4ub x5ub];

% Total number of optimization iterations
totiter = (meshsize+1).^2;

disp('Total number or iterations:')
disp(totiter+1);
disp('--------------------------------------------------------------------------------');

% Vector counter and solution matrix initalizations
count = 1;
desmat = zeros(totiter+1,5);
costmat = zeros(totiter+1,1);
initmat = zeros(totiter+1,5);
massmat = zeros(totiter+1,1);
compmat = zeros(totiter+1,1);
perfmat = zeros(totiter+1,2);

% Define inital values for x(1), x(2), and x(3)
aa = (x1ub-x1lb)./2;
bb = (x2ub-x2lb)./2;
cc = (x3ub-x3lb)./2;

% Call optimization for each inital design vector
for dd = x4lb:x4inc:x4ub;
  for ee = x5lb:x5inc:x5ub;
    % Declare initial design vector
    x = [aa bb cc dd ee];

    % Optimization routine
    [xfinal,costv,exitflag,output,lamda,grad,hess]=fmincon('cost',x,[],[],[],[],...
       xlb,xub,'vacconstraints',options);

    % If optimization routine converges to a solution, assign to solution matrices
    if exitflag >0;
      desmat(count,:) = xfinal;
      costmat(count,1) = costv;
      initmat(count,:) = x;
      perfmat(count,1) = mass(desmat(count,:));
      perfmat(count,2) = 1-(desmat(count,3)/desmat(count,5));
      disp('Feasible solution found:');
      disp(xfinal);
    end

    count = count + 1;
    disp(count);
  end
```

```
end

t=toc;

%%%%%%%%%%%%%%%%%%%%%%%%%%%%%%%%%%%%%%%%%%%%%%%%%%%%%%%%%%%%%%%%%%%%%%%
```

Chord Height Calculation

```
%%%%%%%%%%%%%%%%%%%%%%%%%%%%%%%%%%%%%%%%%%%%%%%%%%%%%%%%%%%%%%%%%%%%%%%
% This function calculates the chord height for the necessary
% deflection for a curved mounting surface defined by specimen radius
% seal diameter and seal cross section diameter; x(3), x(4), x(5)

function fvalue = chordhei(x)

global bendrad

fvalue = bendrad - .5.*(4.*bendrad.^2-(x(4)+x(5)).^2).^.5;
return;

%%%%%%%%%%%%%%%%%%%%%%%%%%%%%%%%%%%%%%%%%%%%%%%%%%%%%%%%%%%%%%%%%%%%%%%
```

Cost Function (Mass)

```
%%%%%%%%%%%%%%%%%%%%%%%%%%%%%%%%%%%%%%%%%%%%%%%%%%%%%%%%%%%%%%%%%%%%%%%
% Cost function
% this script uses the following design vector to determine the mass
% of the attachment fixture.
% des.vec. syntax ==> ( tc, tw, tg, ds, cs)

function fvalue = cost(x);

global rhocup rhoseal emodcup normalmass alpha armmass poiscup

fvalue=(pi.*rhocup.*((x(4)./2+2.*x(2)+x(5)).^2.*(x(3)+x(1))-(x(4)./2).^2.*x(3)-...
   (((x(4)./2)+x(2)+x(5)).^2-(x(4)./2+x(2)).^2).*x(3))+...
   (2.*pi.^2.*(x(5)./2).^2*((x(4)+x(5))./2)).*rhoseal);

return;

%%%%%%%%%%%%%%%%%%%%%%%%%%%%%%%%%%%%%%%%%%%%%%%%%%%%%%%%%%%%%%%%%%%%%%%
```

Maximum Vacuum Generated Load

```
%%%%%%%%%%%%%%%%%%%%%%%%%%%%%%%%%%%%%%%%%%%%%%%%%%%%%%%%%%%%%%%%%%%%%%%
% This function calculates the maximum sealing force of the cup
% using the design vector and the design constant "maxvac"

function fvalue = maxload(x)

global maxvac
```

```
fvalue = pi.*((x(4)+x(5))./2).^2.*maxvac;

return;

%%%%%%%%%%%%%%%%%%%%%%%%%%%%%%%%%%%%%%%%%%%%%%
```

Seal Compression Load Calculation

```
%%%%%%%%%%%%%%%%%%%%%%%%%%%%%%%%%%%%%%%%%%%%%%%%%%
% Script calculates seal compressive load per linear inch of seal when
% given seal cross section diameter and maximum compression.
% function uses variables x(3) and x(5)

function fvalue=sealload(x)

% The below values were taken form Parkers O-ring Design Handbook, and
% represent compression load in pounds per linear inch of o-ring for
% compression percentages of:
% 5% 10% 20% 30% 40%
% The loads are then converted to Newtons per linear meter of seal.

f070=[.45 1.2 2.6 6 15];
fm070 = f070.*4.448.*39.37;

f103=[.45 1.6 5.4 10 22];
fm103 = f103.*4.448.*39.37;

f139=[.45 1.1 2.7 6 17];
fm139 = f139.*4.448.*39.37;

f210=[2 5 11 20 45];
fm210 = f210.*4.448.*39.37;

f275=[2 5 15 28 70];
fm275 = f275.*4.448.*39.37;

def=[.05 .1 .2 .3 .4];

%Fit as 2nd order
stiff070=polyfit(def,fm070,2);
stiff103=polyfit(def,fm103,2);
stiff139=polyfit(def,fm139,2);
stiff210=polyfit(def,fm210,2);
stiff275=polyfit(def,fm275,2);

if x(5) < .0022
   stiff = stiff070;
elseif x(5) >= .0022 & x(5) < .0031
   stiff = stiff103;
elseif x(5) >= .0031 & x(5) < .0044
   stiff = stiff139;
elseif x(5) >= .0044 & x(5) < .0061
   stiff = stiff210;
elseif x(5) >= .0061
```

```
    stiff = stiff275;
end
compmax = 1-(x(3)./x(5));

fvalue = (polyval(stiff,compmax));

%%%%%%%%%%%%%%%%%%%%%%%%%%%%%%%%%%%%%%%%%%%%%%%%%%%%%%%%%%%%%%%%%%%%%%%%%%%%%%%%%%%
```

Optimization Constraints

```
%%%%%%%%%%%%%%%%%%%%%%%%%%%%%%%%%%%%%%%%%%%%%%%%%%%%%%%%%%%%%%%%%%%%%%%%%%%%%%%%
% this script contains the constraints for the fixture optimization

function [g,dummy1] = vacconstraints(x);
global compmax compmin heichord emodcup rhocup rhoseal poiscup maxshak maxvac armmass
dummy1=[];
h = chordhei(x);
stiffcon = sealload(x);
fv = maxload(x);
g = zeros(8,1);

%Constraints

% Natural Frequency Constaint
g(1) = 500 - (2.*((rhocup.*x(1).*pi.*(x(4)./2-x(2)).^2./armmass).^.5)./(pi.*(x(4)./2-...
    x(2)).^2)).*((emodcup.*(x(1).^2)./(12.*rhocup.*(1-poiscup.^2))).^.5);

% Sealing load constraint
g(2) = maxshak - fv + stiffcon.*(pi.*(x(4)+x(5)));

% Radial stress constraint
g(3) = 6.*0.0796.* maxshak ./ (x(1)).^2 - 68.9E6;

% Minimum wall (gland wall) thickness constraint
g(4) = .0015875 - x(2);

% Minimum wall (cup wall) thickness constraint
g(5) = .00079375 - x(1);

% Maximum seal compression constraint
g(6) = 1 - (x(3)./x(5)) - .4;

% Minimum seal compression constraint
g(7) = .05 - 1 + (x(3)./x(5)) + (h./x(5));

% Minimum seal deflection constraint
g(8) = (1.7e-4) - .05 * x(5);

%%%%%%%%%%%%%%%%%%%%%%%%%%%%%%%%%%%%%%%%%%%%%%%%%%%%%%%%%%%%%%%%%%%%%%%%%%%%%%%%%%%%%%%%%%%%%%
```